Recent Results from HADES

Christoph Blume
for the HADES Collaboration
GOETHE UNIVERSITÄT FRANKFURT AM MAIN

58th International Winter Meeting on Nuclear Physics

Bormio, Italy, Jan. 20. – 24., 2020

HADES
The Physics Program

Open questions
Origin of hadron masses
Role of of condensates
QCD-Confinement
Equation-of-state of dense matter

Super-dense matter in the laboratory

Neutron Star Merger
Observation via gravitational waves

GW170817: B.P. Abott et al. (LIGO + VIRGO)
PRL **119** (2017) 1611001

Sensitivity to equation-of-state

Super-dense matter in the universe

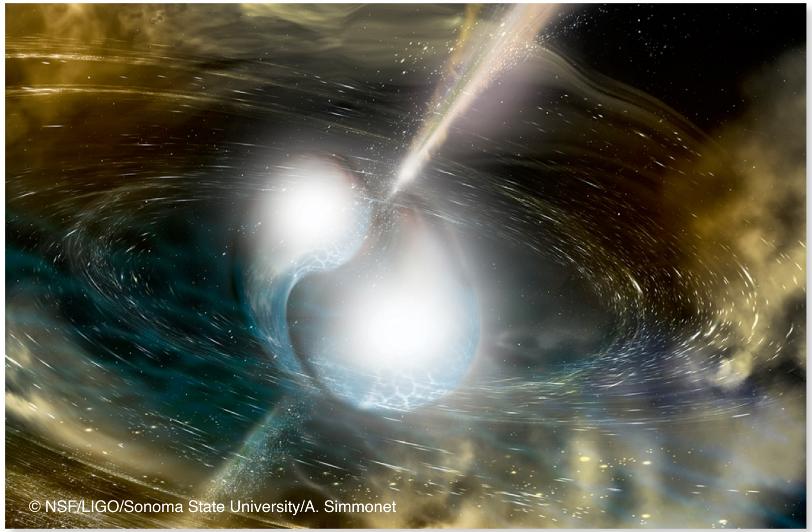

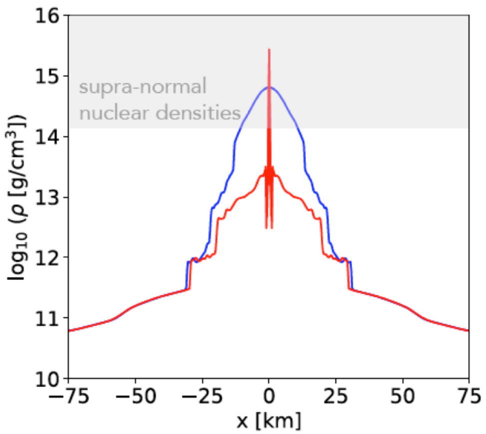

Density profile across a merging NS binary system. Taken $t = 1.4$ ms ($t = 0$ see below).

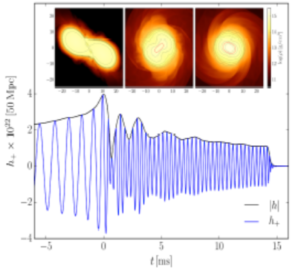

M. Hanauske, L. Rezzolla et al. J.Phys.Conf.Ser. 878 (2017) no.1, 012031

HADES
The Physics Program

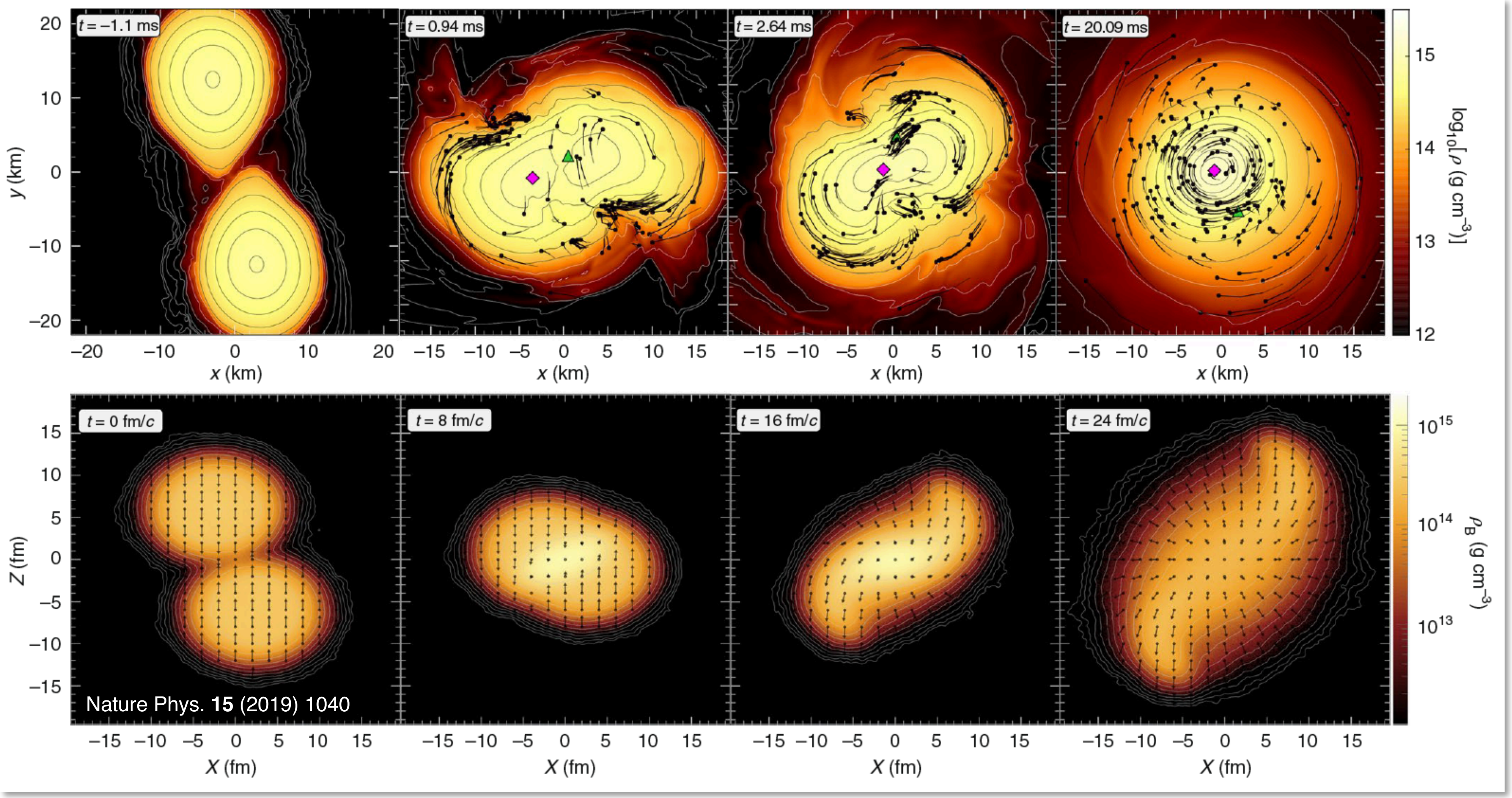

Nature Phys. **15** (2019) 1040

HADES
The Physics Program

Heavy-ion collisions
QCD phase diagram in the region of high μ_B

Rare and penetrating probes

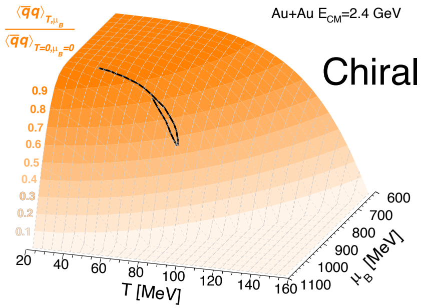

Chiral condensate

F. Seck et al.,
JPCS **024** (2018) 012011

Bulk properties of dense fireball

Pion + proton beams
Properties of baryon resonances
(vacuum, cold QCD matter)

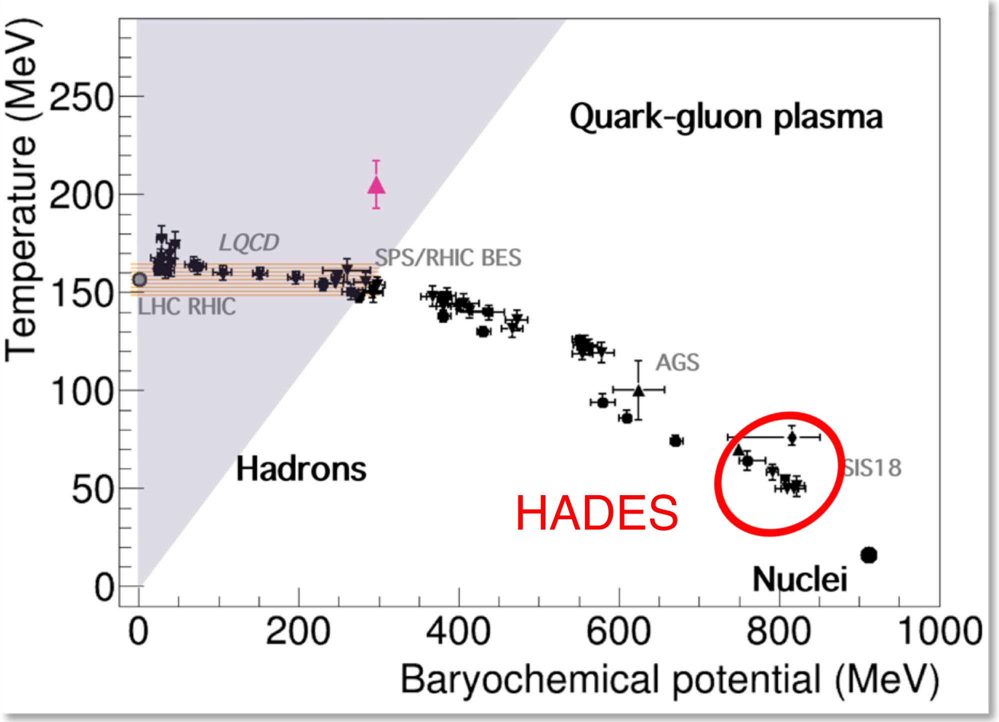

HADES

The Experiment

Fast detectors

Trigger rates up to 50 kHz

Large acceptance

Full azimuthal angle

Polar angle coverage: 18° – 85°

Segmented Au target

2% Interaction probability

Very low material budget

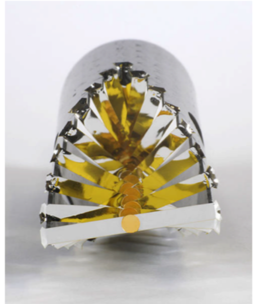

Particle identification

Time-of-flight (TOF + RPC)

dE/dx (MDC + TOF)

Cherenkov-effect (RICH)

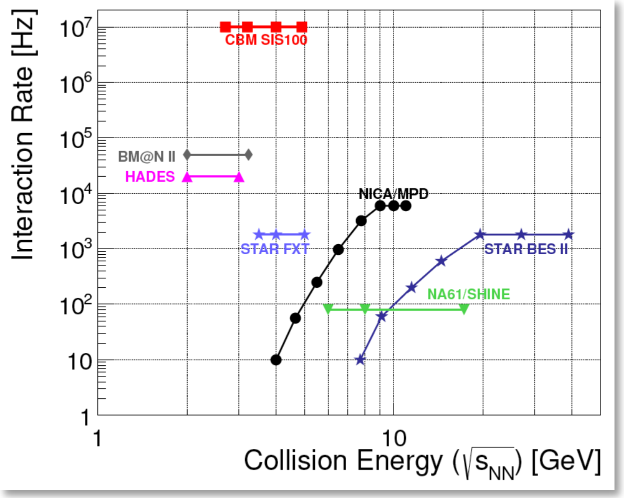

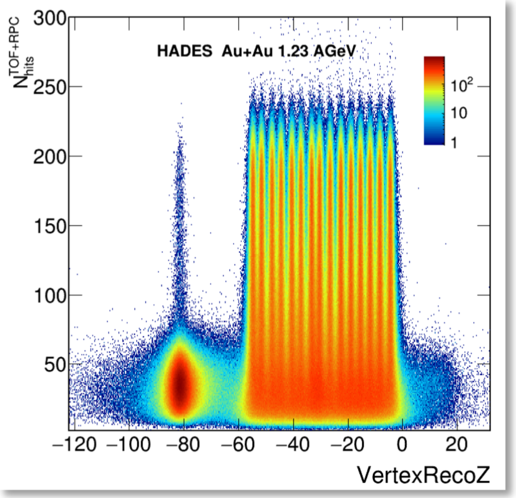

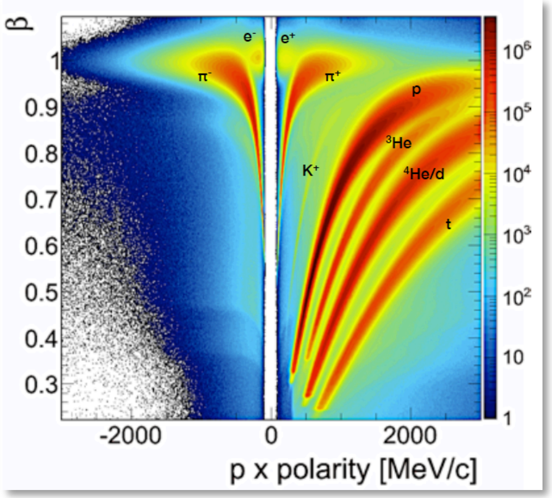

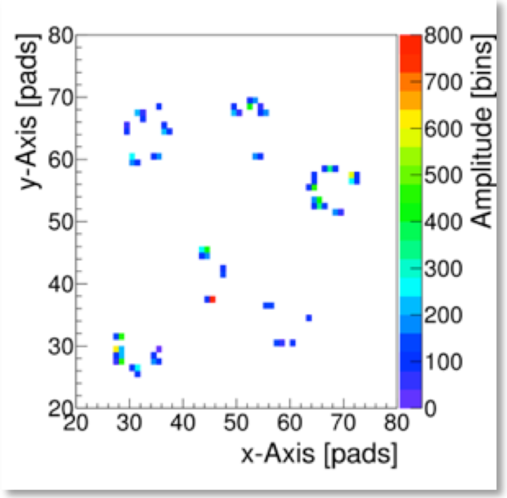

HADES

The Experiment

Au+Au at $\sqrt{s_{NN}}$ = 2.42 GeV

Beam: 1.5 x 10^6 ions / s
7 x 10^9 events recorded
LVL1 trigger: 40% most central

Centrality selection

N_{hits} in TOF+RPC
(standard analysis)

Sum of charges in Forward Wall Σ_Q
(E-by-e fluctuation analysis)

Volume determination

N_{part} from Glauber MC

Eur. Phys. J. **A54** (2018) 85

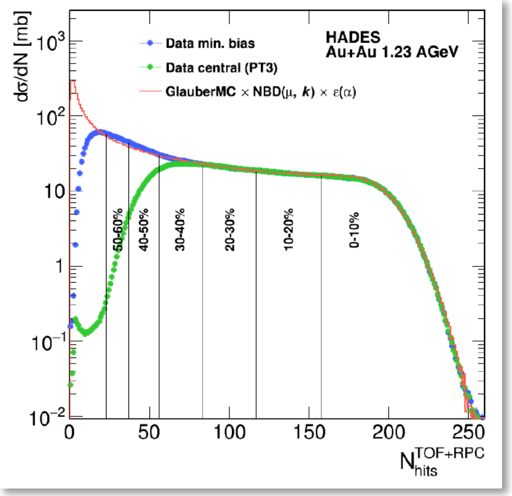

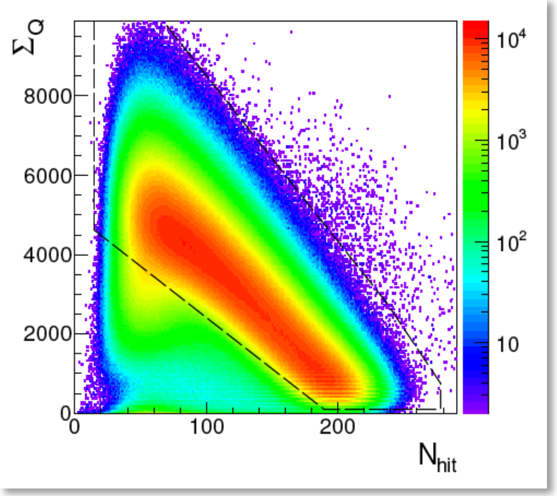

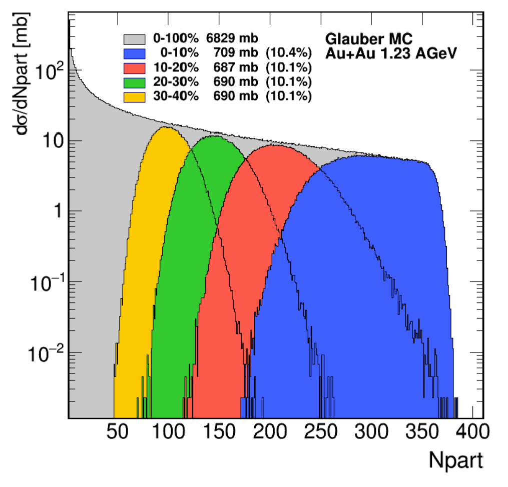

HADES

The Experiment

Event plane Reconstruction

1^{st}-Order event plane

Projectile spectators in Forward Wall

EP-resolution via sub-event method

J.-Y. Ollitrault, arXiv:nucl-ex/9711003

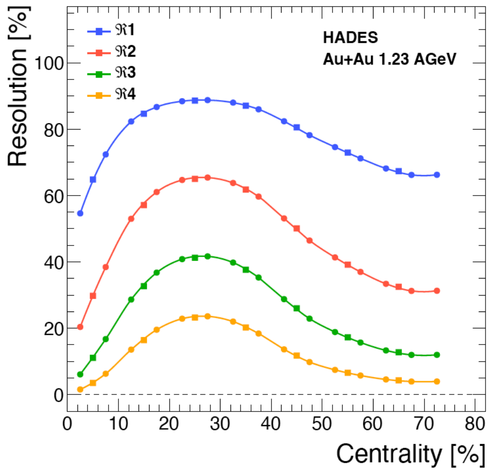

$$v_n = v_n^{obs} \,/\, \mathfrak{R}_n$$

$$\mathfrak{R}_n = \langle \cos[n(\Psi_n - \Psi_{RP})] \rangle$$

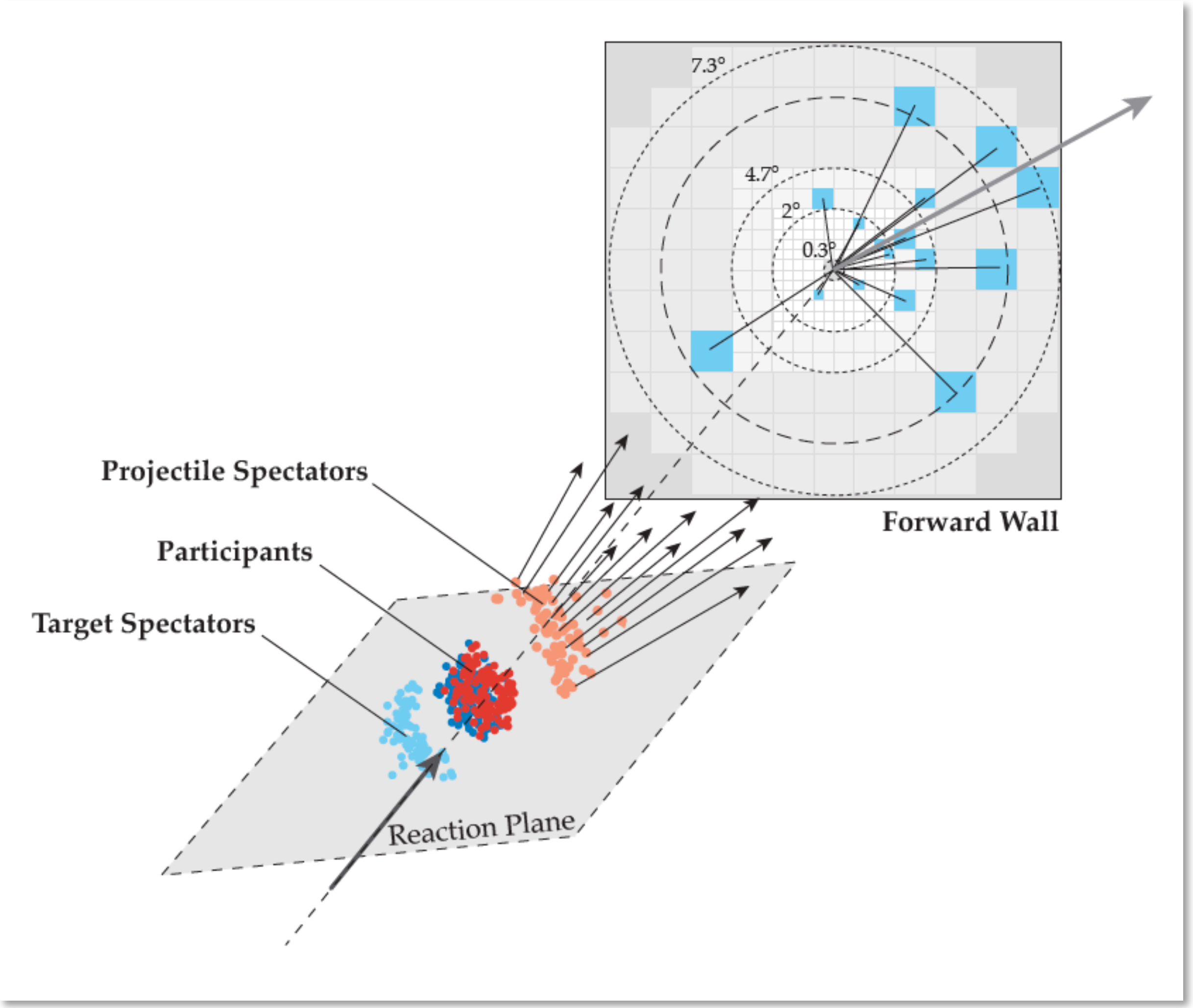

HADES

The Experiment

Au+Au at 1.23*A* GeV
($\sqrt{s_{NN}}$ = 2.42 GeV)

Particle production
Virtual photons
Collective effects
Femtoscopy
Global Λ polarization
Proton number fluctuations

π^- + N at 1.7 GeV

Strangeness in cold nuclear matter

Ag+Ag at 1.58*A* GeV
($\sqrt{s_{NN}}$ = 2.6 GeV)

FAIR Phase-0: first look

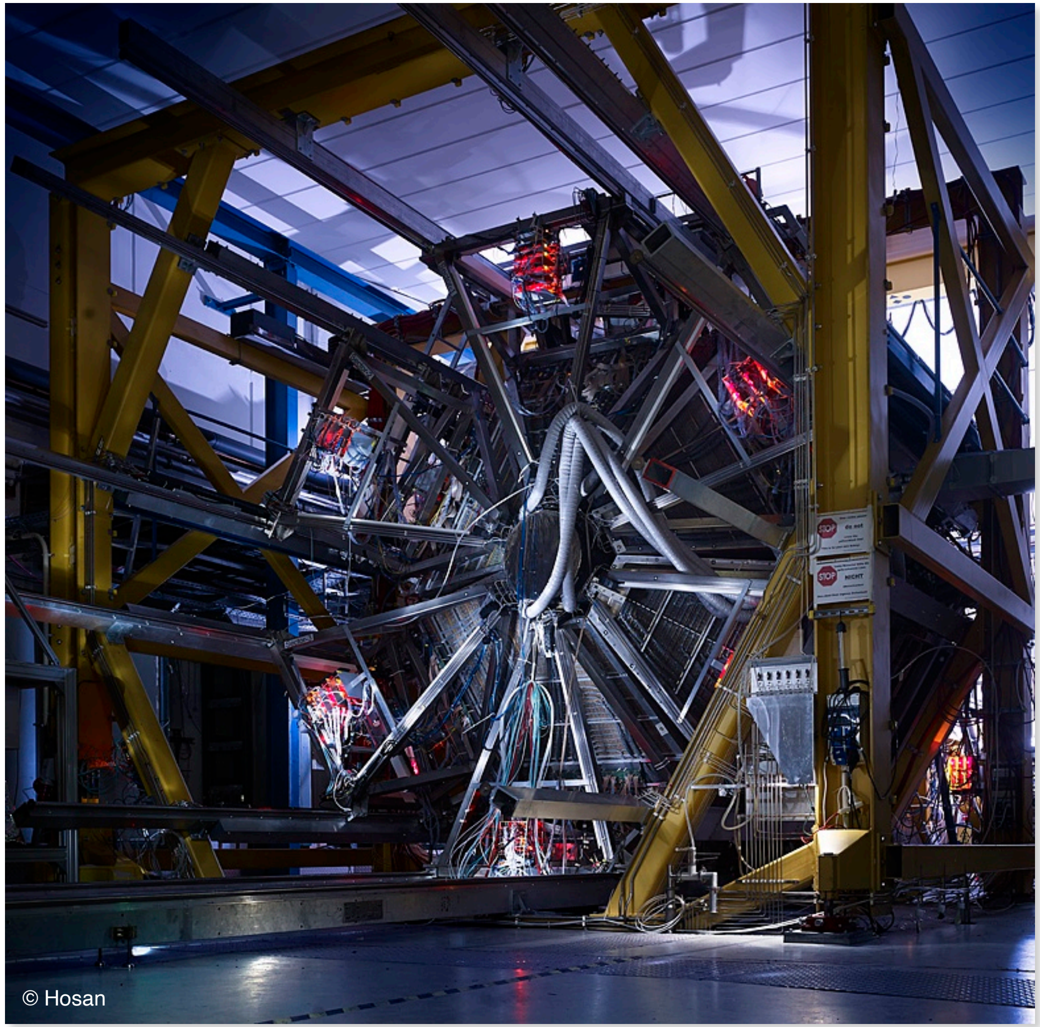

Particle Production

Strange Particles: K^0_s and Λ

Weak decay topology

Large phase space coverage

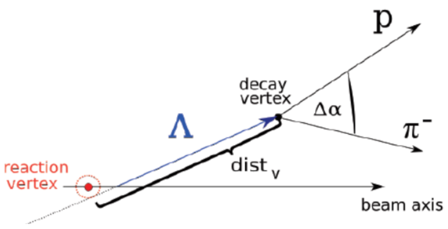

New developments

Further improvements with ANN

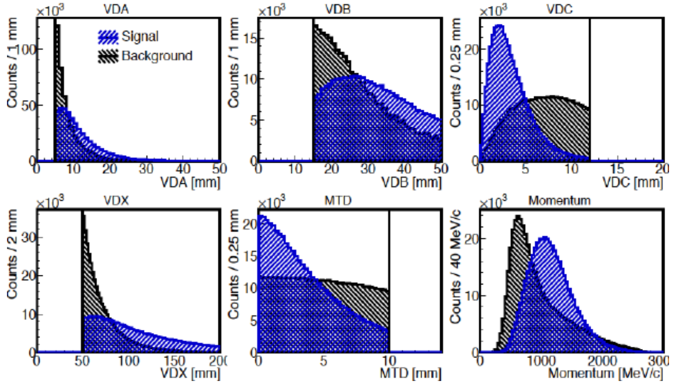

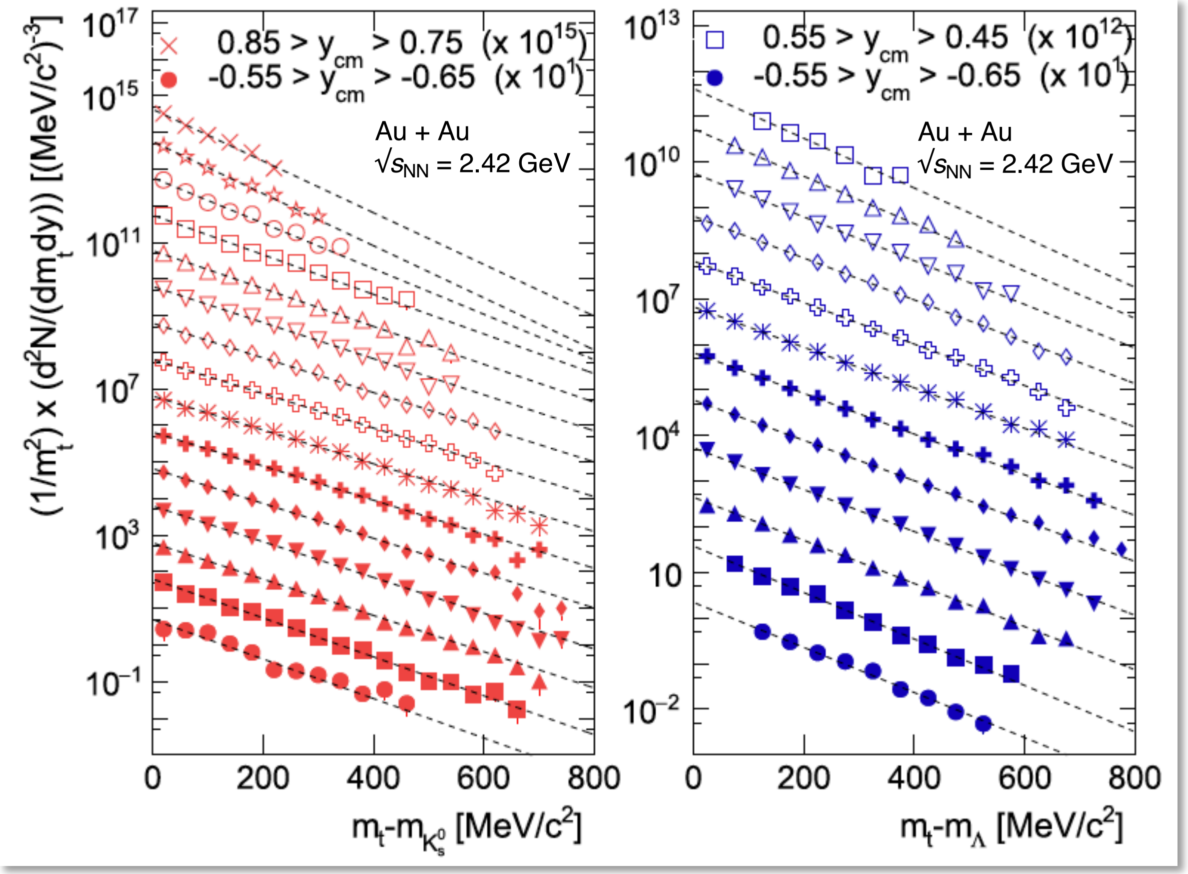

Phys. Lett. **B793** (2019) 457

Particle Production

Strange Particles: K^0_s and Λ

Sub-threshold production

No strangeness production in elementary NN-collisions at $\sqrt{s_{NN}}$ = 2.4 GeV
(Lowest thres.: NN ⟶ NΛK⁺ $\sqrt{s_{NN}}$ = 2.55 GeV)

Sensitive to system properties

Energy transfer via strangeness exchange
(π Y ⟶ N K⁻)
Coupling of K⁻ to baryons
Potentials: K⁺N repulsive, K⁻N attractive

Steep excitation function

Phys. Lett. **B793** (2019) 457

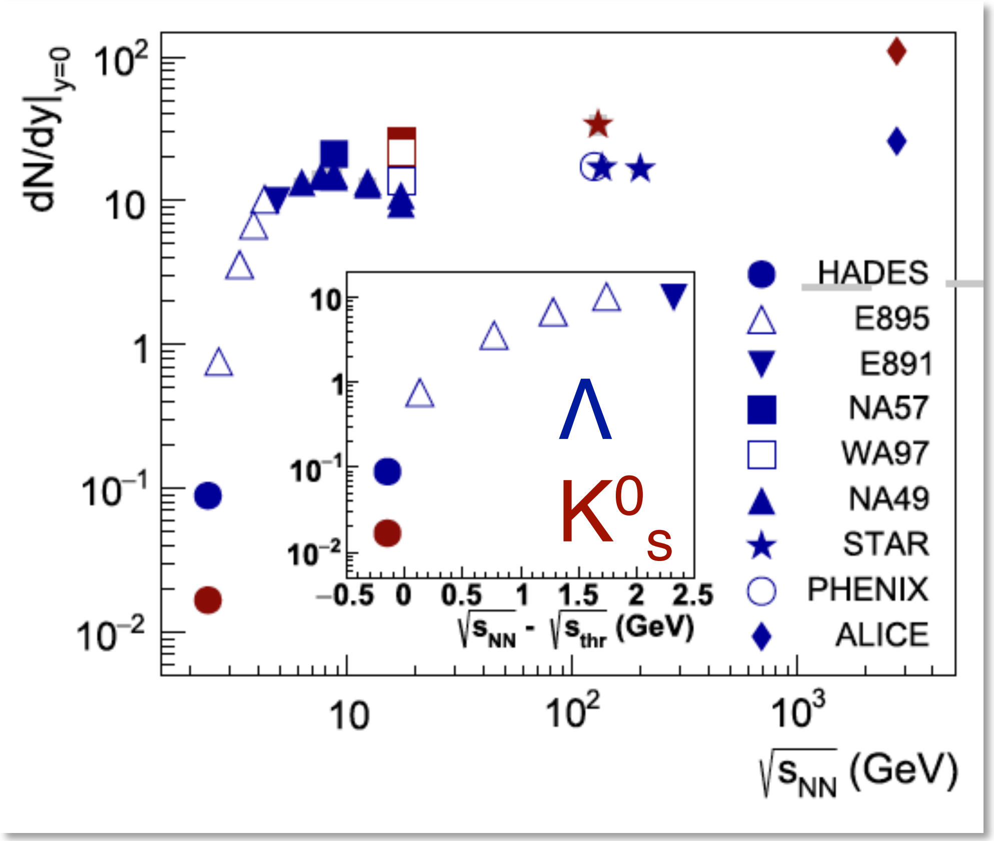

Data compilation: CB and C. Markert, Prog. Part. Nucl. Phys. **66** (2011) 834

Particle Production

Strange Particles: System Size Dependence

Sub-threshold production

No strangeness production in elementary NN-collisions at $\sqrt{s_{NN}}$ = 2.4 GeV
(Lowest thres.: NN ⟶ NΛK+ $\sqrt{s_{NN}}$ = 2.55 GeV)

System size dependence

Parameterization: $\langle Mult \rangle \sim \langle A_{part} \rangle^{\alpha}$
Multiplicities rise stronger than linear ($\alpha > 1$)

Universal A_{part} dependence

Expected hierarchy due to different thresholds not seen

Phys. Lett. **B793** (2019) 457

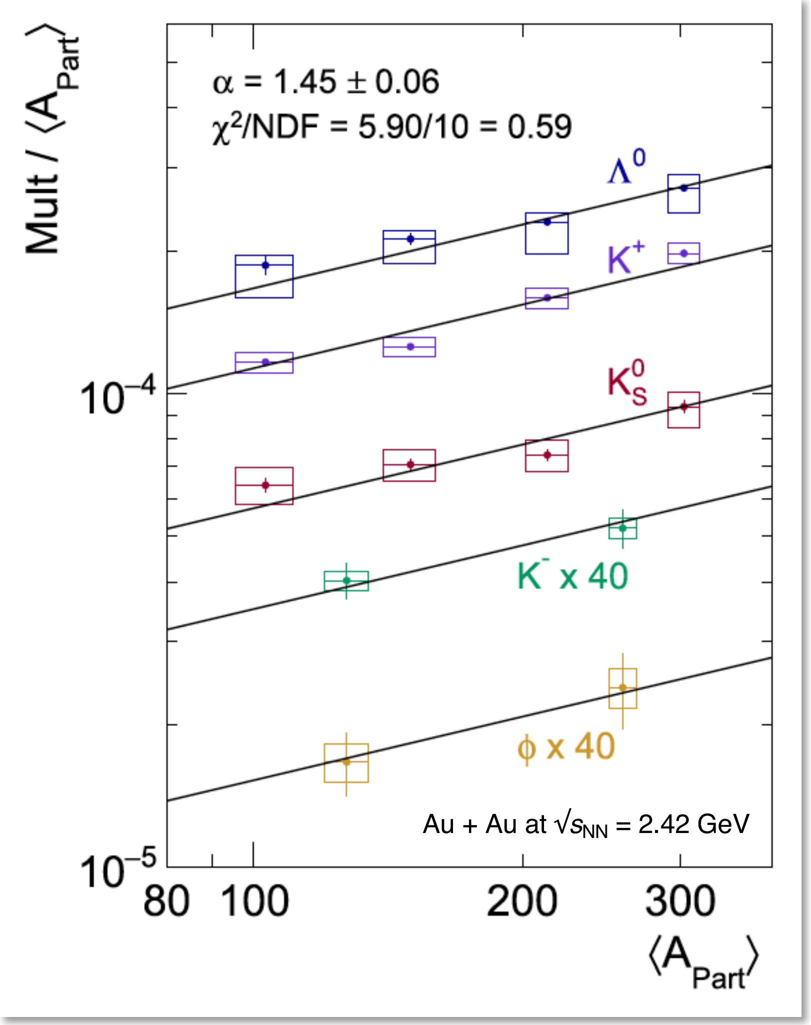

Particle Production

Strangeness in Cold Matter: Pion-Nucleus

Pion beam facility

Secondary π^- beam at 1.7 GeV/c
Intensity: ~ $3 \cdot 10^5$ π^-/s

CERBEROS tracking system: 0.3%(σ) res.
Eur. Phys. J. **A53** (2017) 188

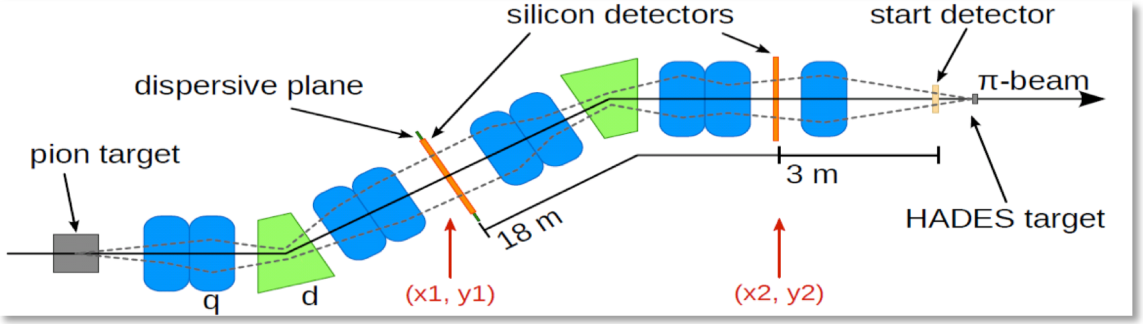

Target nuclei: C and W

Comparison of K^+, K^- and ϕ production
Phys. Rev. Lett. **123** (2019) 022002

π-induced production close to surface
⟶ Long path lengths inside nuclear matter

Study of absorption in cold nuclear matter

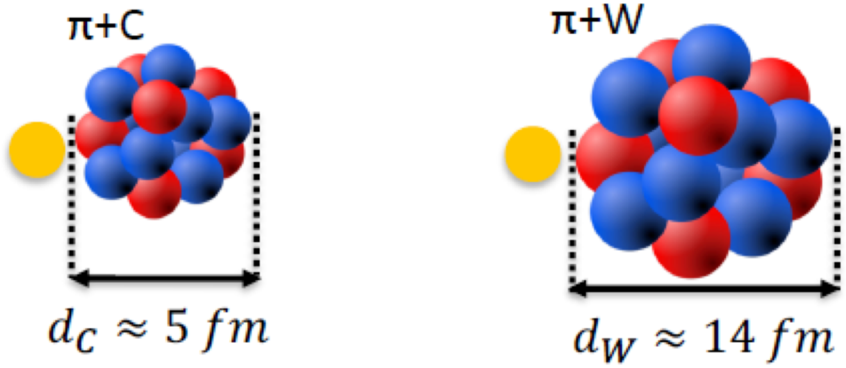

Mean free path: $\lambda_\pi \approx 1.5$ fm

Particle Production

Strangeness in Cold Matter: Pion-Nucleus

Suppression of K⁻ relative to K⁺

Average value (in HADES acceptance):

$$(K^-/K^+)_W/(K^-/K^+)_C = 0.319 \pm 0.009(\mathrm{stat})^{+0.014}_{-0.012}(\mathrm{syst})$$

Suppression of ϕ

ϕ/K⁻ ratios comparable in π+C and π+W:

$$(\phi/K^-)_C = 0.55 \pm 0.04(stat)^{+0.06}_{-0.07}(sys)$$

$$(\phi/K^-)_W = 0.63 \pm 0.06(stat) \pm 0.11(sys)$$

⟶ Similar suppression for ϕ than for K⁻

In line with measured transparency ratio:

$$T = [(12/184)(\Delta\sigma^{\phi}_{W}/\Delta\sigma^{\phi}_{C})]$$
$$= 0.18 \pm 0.02 \pm 0.01^{+0.04}_{-0.03}$$

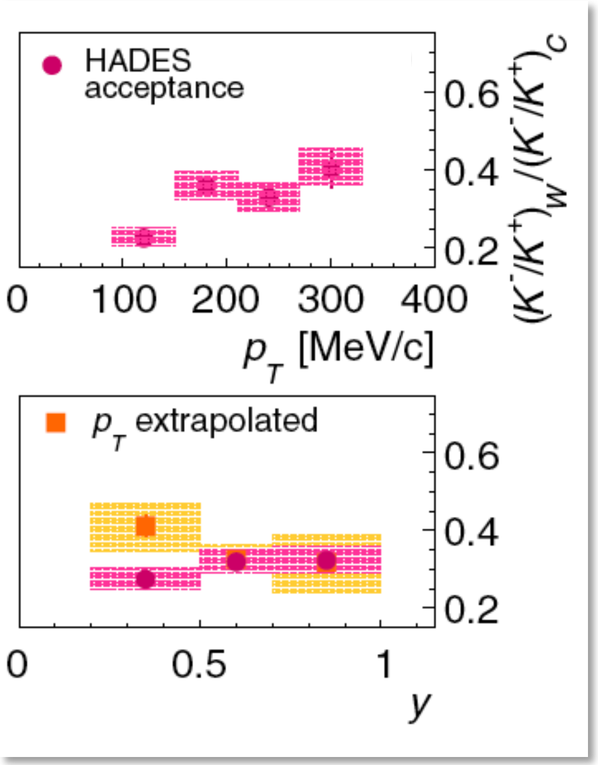

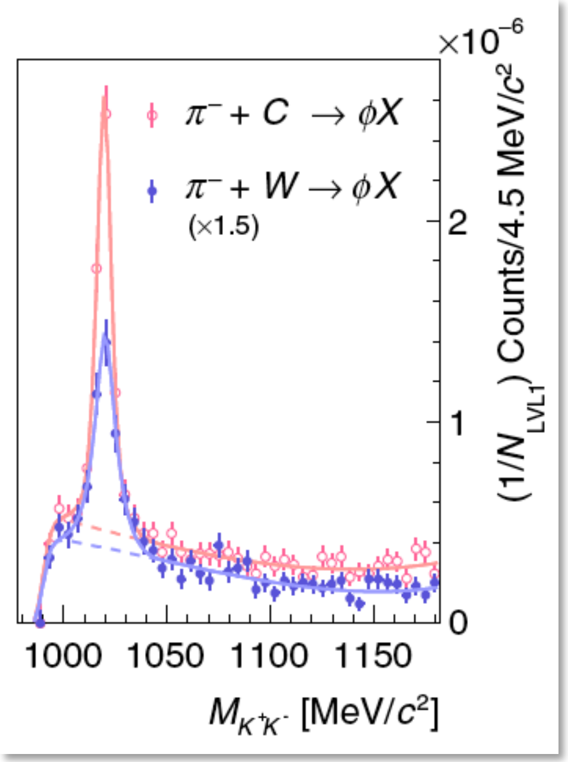

Phys. Rev. Lett. **123** (2019) 022002

Particle Production

Protons, Deuterons and Tritons

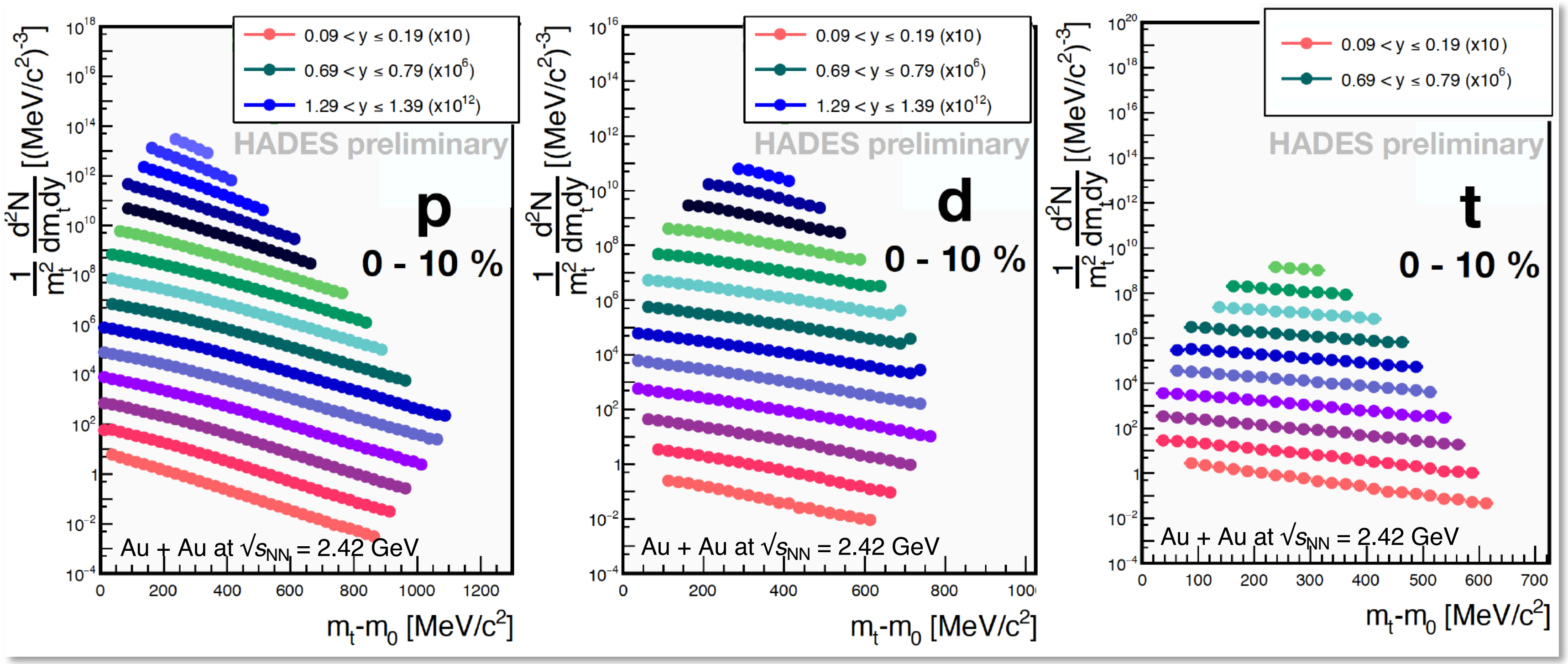

New high statistics data on protons and light nuclei

Multi-differential analysis

M. Szala, SQM19

Particle Production

Transverse Mass Spectra ⟶ Kinetic Freeze-Out

Fit with Blast-Wave model

Phys. Rev. **C48** (1993) 2462

π, p, K, Λ, ϕ: T_{kin} = 62 ± 10 MeV

$\langle \beta_T \rangle$ = 0.36 ± 0.04

Light nuclei:: T_{kin} = 71 ± 8 MeV

$\langle \beta_T \rangle$ = 0.30 ± 0.02

World systematics

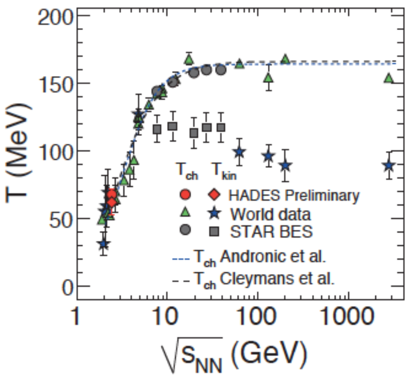

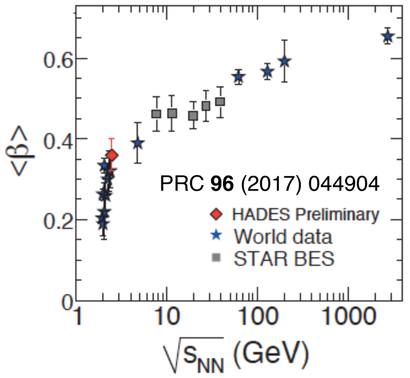

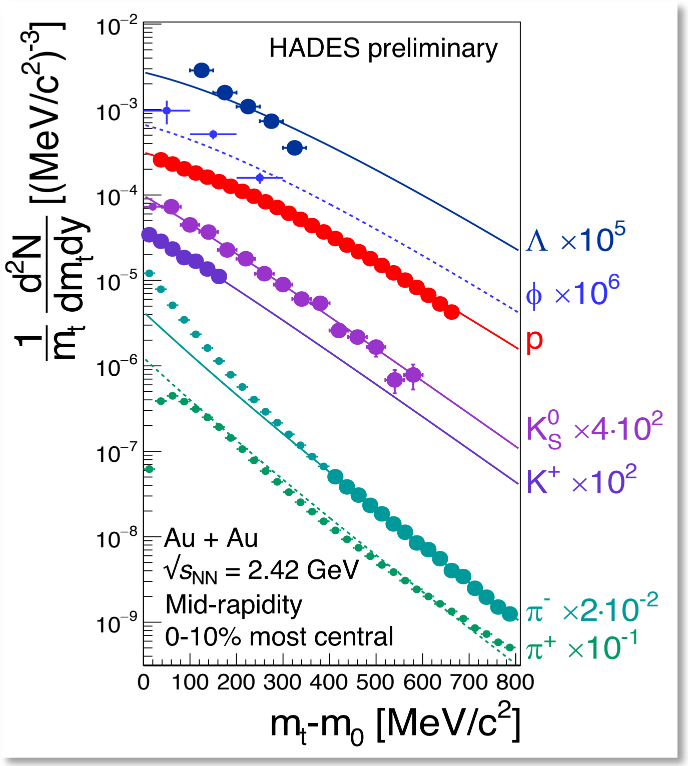

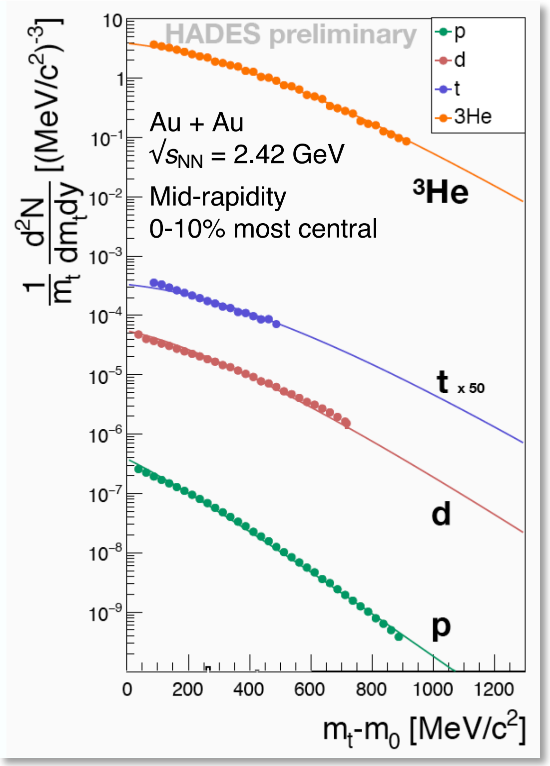

Blast-Wave model

⟹ Kin. freeze-out params.:

Temperature: T_{kin}

Average transverse expansion velocity: $\langle \beta_T \rangle$

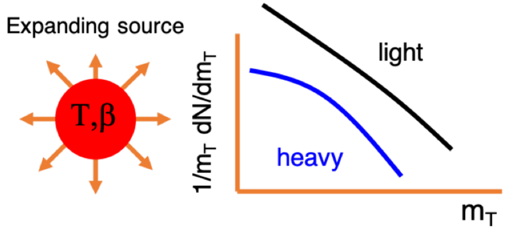

M. Szala, ECT* Workshop

Particle Production

Particle Yields ⟶ Chemical Freeze-Out

Fit with THERMAL-FIST

Freeze-Out parameters (T_{chem}, μ_B) follow universal chemical freeze-out curve

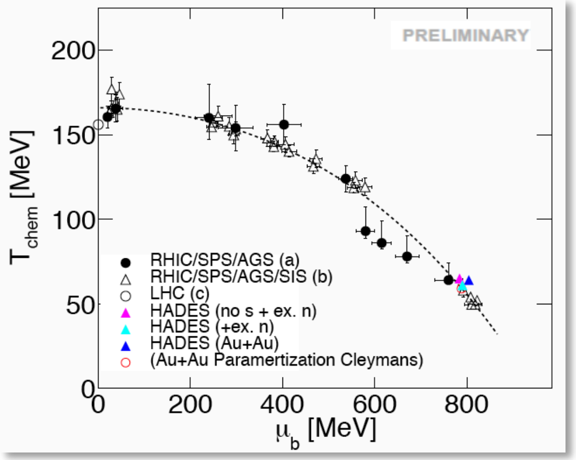

Freeze-out points
J. Cleymans, H. Oeschler and K. Redlich, Phys. Rev. **C59** (1999)
R. Averbeck, R. Holzmann, V. Metag and R.S. Simon, Phys. Rev. **C67** (2003)

Relatively high χ^2 for full hadron spectrum

Inclusion of excited nuclei states helps
Add. exclusion of strangeness ⇒ small χ^2
(see backup slides)

Thermal Fist: V. Vovchenko H. Stoecker, Comput. Phys. Commun. 244 (2019) 295.

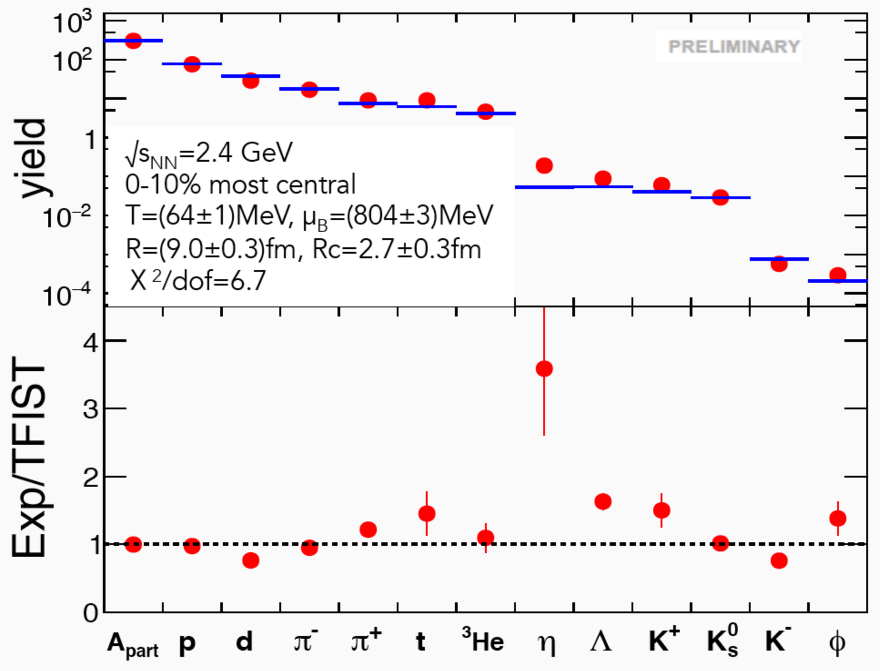

M. Lorenz,
EMMI-Workshop on Anti-matter, hyper-matter and exotica

Virtual Photons

Di-Electron Spectrum

1^{st} heavy system at low $\sqrt{s_{NN}}$

Two analysis strategies

Efficiency corrected

Nature Phys. **15** (2019) 1040

Large excess radiation

$0.15 < M_{ee} < 0.7$ GeV/c^2

Relative to meson decays and NN reference

$$\frac{dN^{NN}_{ref}}{dM_{ee}} = \left(0.54\frac{dN^{pp}}{dM_{ee}} + 0.46\frac{dN^{np}}{dM_{ee}}\right)\langle A_{part}\rangle$$

Subtraction of reference

Extraction of spectrum of excess radiation

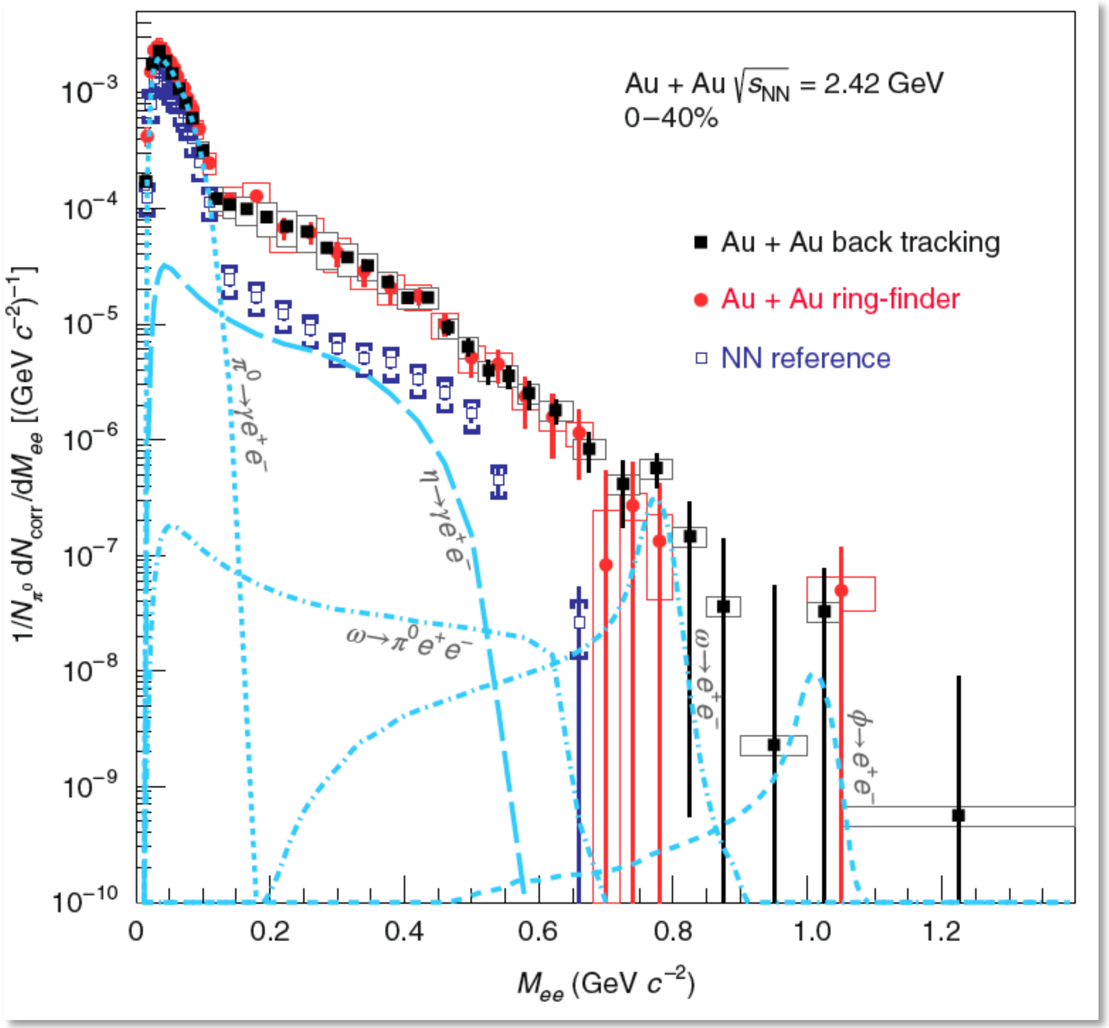

Virtual Photons

Di-Electron Spectrum

Spectrum of excess radiation

Not described with vacuum ρ

Broadening of ρ due to ρ-baryon scattering

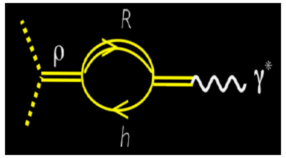

Thermal radiation of medium

Thermal radiation folded with fireball evolution from coarse-grained transport

In-medium propagator: R. Rapp and H. van Hees, PLB **753** (2016) 586
ρ – a₁ chiral mixing: R. Rapp and P. Hohler, PLB **731** (2014) 103
CG FRA: S. Endres et al., PRC **92** (2015) 014911
CG GSI-TAMU: T. Galatyuk, F. Seck et al., EPJA **52** (2016) 131
CG SMASH: J. Staudenmaier et al., PRC **98** (2018) 054908.
HSD transport model: E. Bratkovskaya et al., PRC **87** (2013) 064907.

Exponential spectrum ⟶ black body rad.

Fit result: T_{rad} = 71.8 ± 2.1 MeV

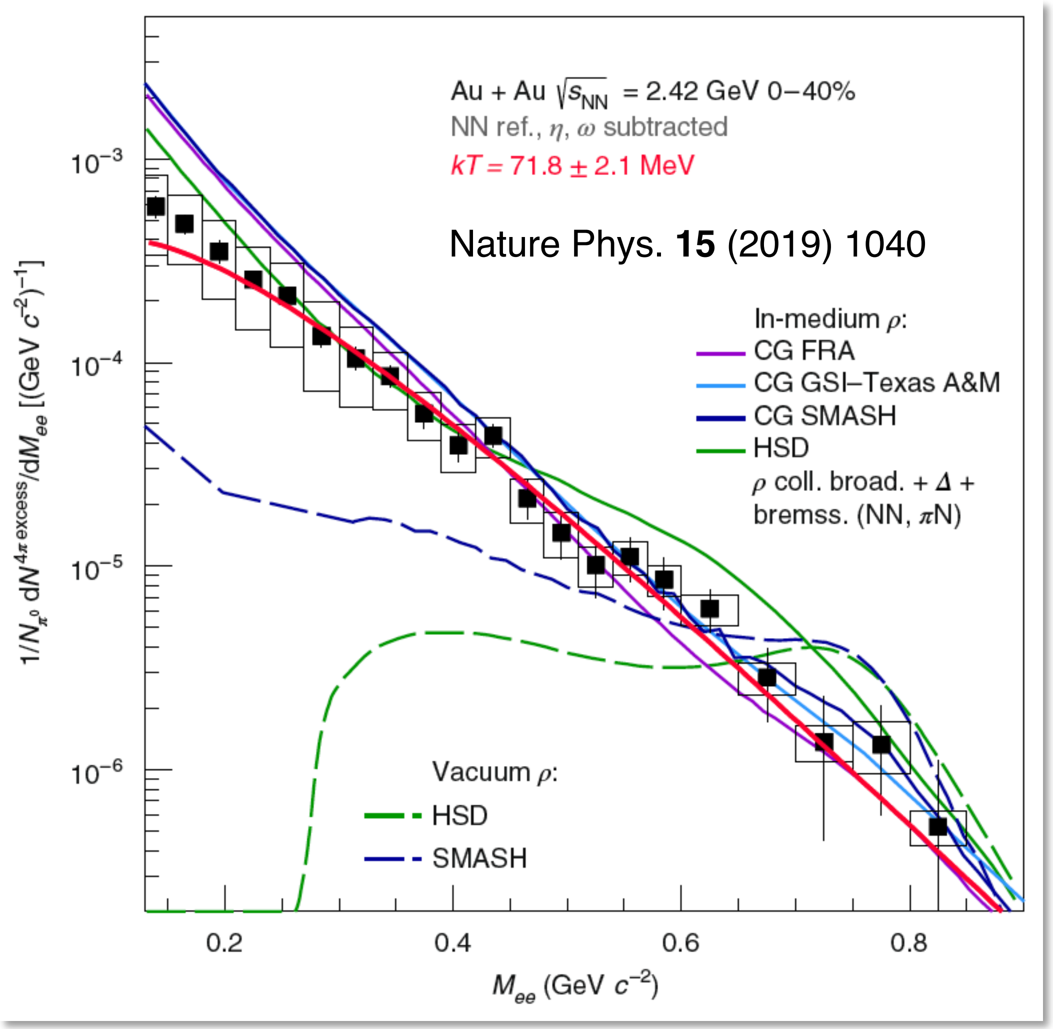

Virtual Photons

Di-Electron Spectrum

Thermal radiation of medium

Exponential spectrum ⟶ black body rad.
Fit result: T_{rad} = 71.8 ± 2.1 MeV

QCD phase diagram

3rd data point from HADES
$T_{rad} > T_{chem} \approx T_{kin}$

SPS measurement by NA60

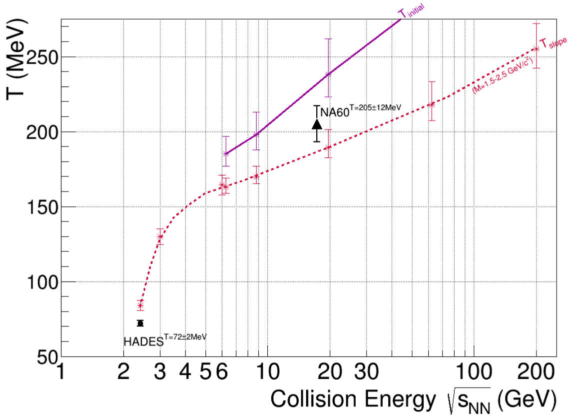

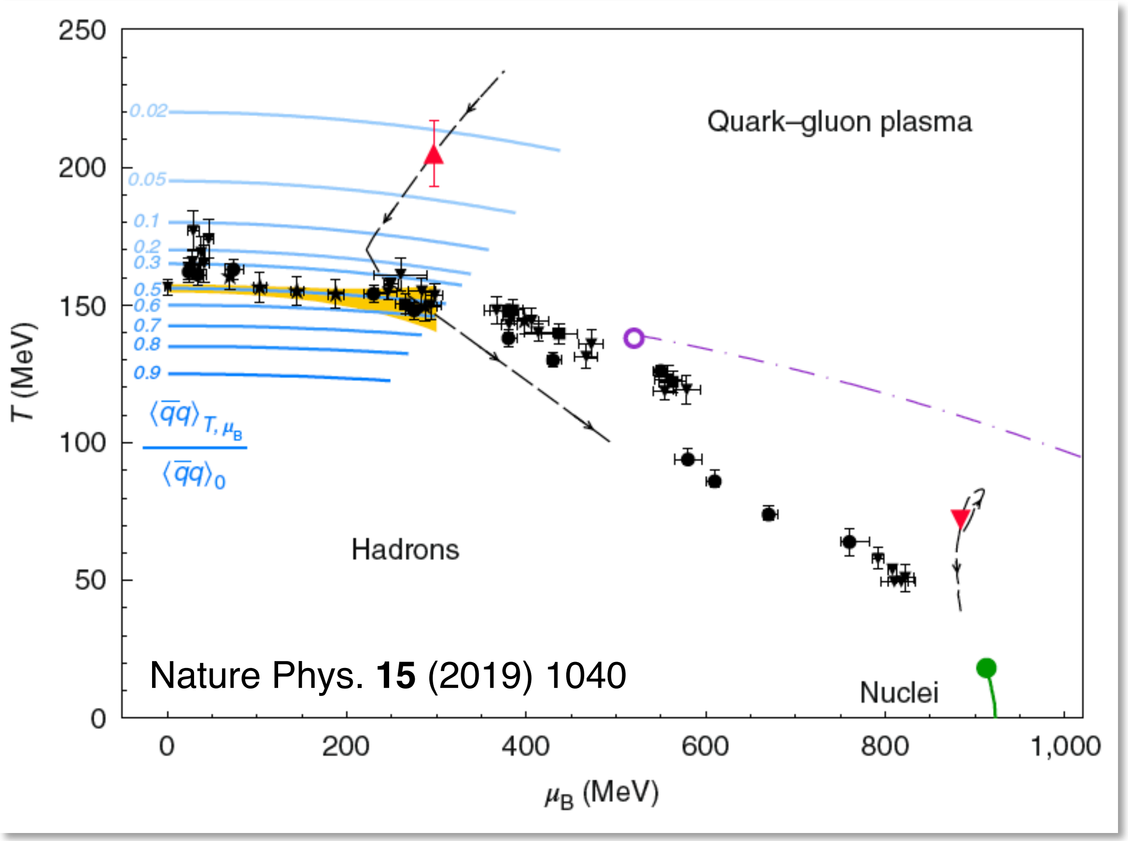

Collective Effects
Principle

Emission relative to event plane
Interactions in medium $\Longrightarrow$ different pressure gradients in different directions

Access to medium properties, e.g. viscosity
Equation-of-state

Fourier-Decomposition
Extraction of moments v_n

$$E\frac{d^3N}{d^3\mathbf{p}} = \frac{1}{2\pi}\frac{d^2N}{p_t dp_t dy}\left(1 + 2\sum_{n=1}^{\infty} v_n \cos[n(\varphi - \Psi_{RP})]\right)$$

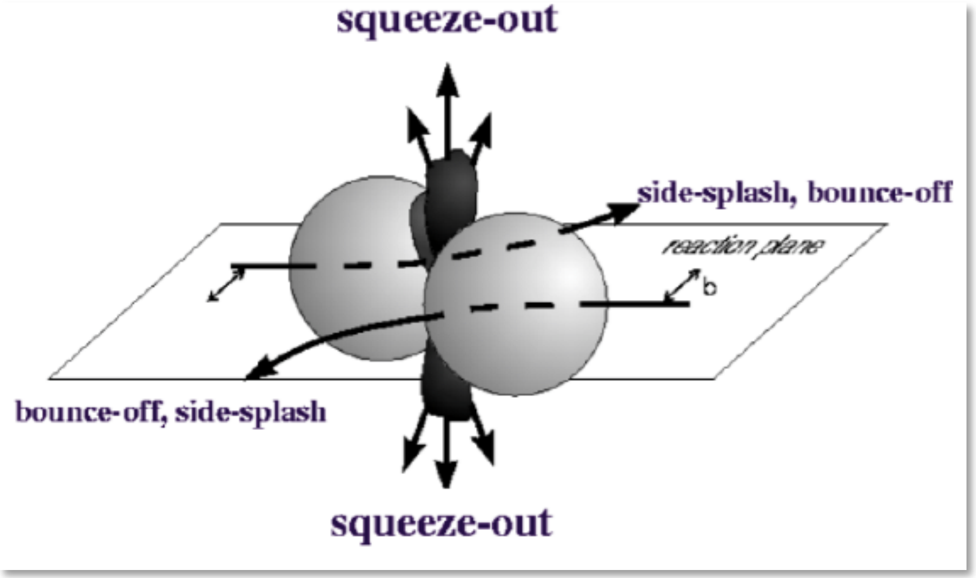

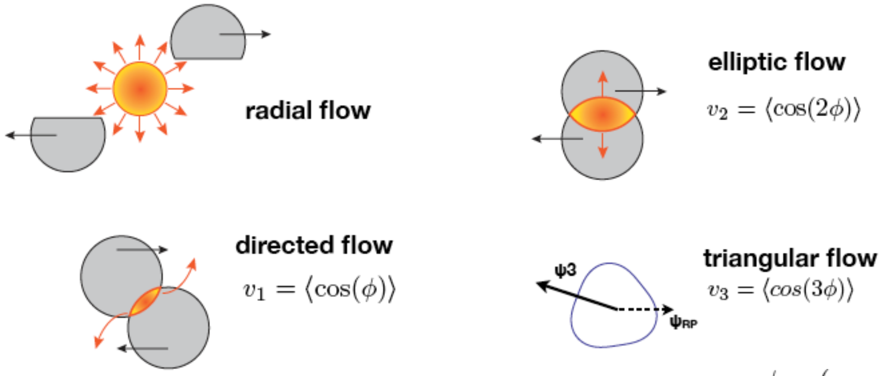

$\phi = (\varphi - \Psi_{RP})$

Collective Effects

Energy Dependence

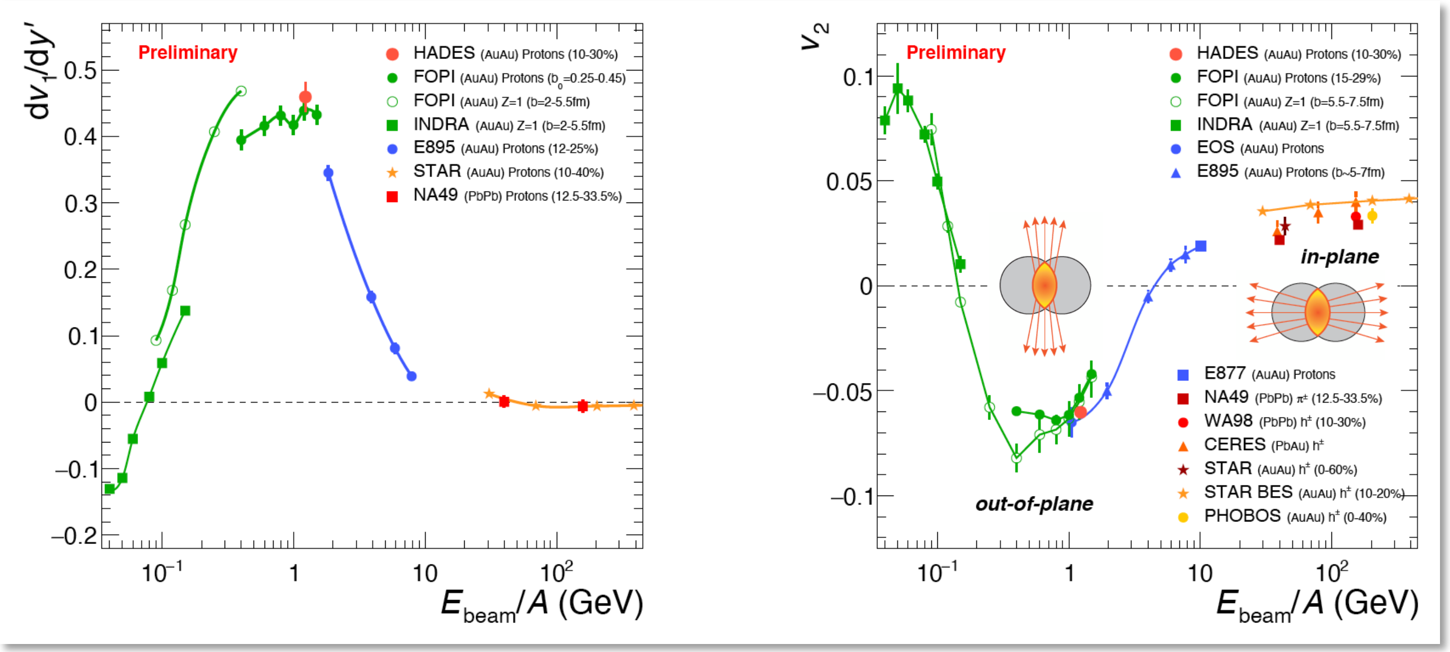

Comparison to world data

Good agreement of integrated dv_1/dy (directed flow) and v_2 (elliptic flow)

Out-of-plane v_2

Long spectator passing time $\tau_{passing} \approx \tau_{expansion} \Longrightarrow$ “squeeze-out”

B. Kardan, QM18

Collective Effects

Results on v_1, v_2, v_3 and v_4 for Protons, Deuterons and Tritons

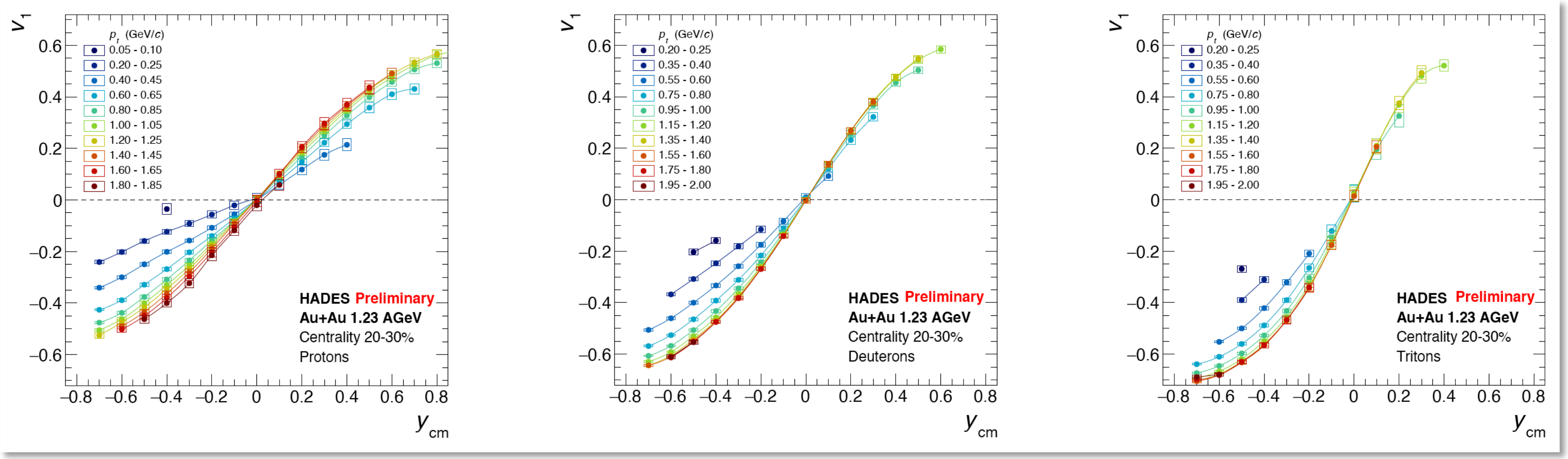

B. Kardan,
QM18

Collective Effects

Results on v_1, v_2, v_3 and v_4 for Protons, Deuterons and Tritons

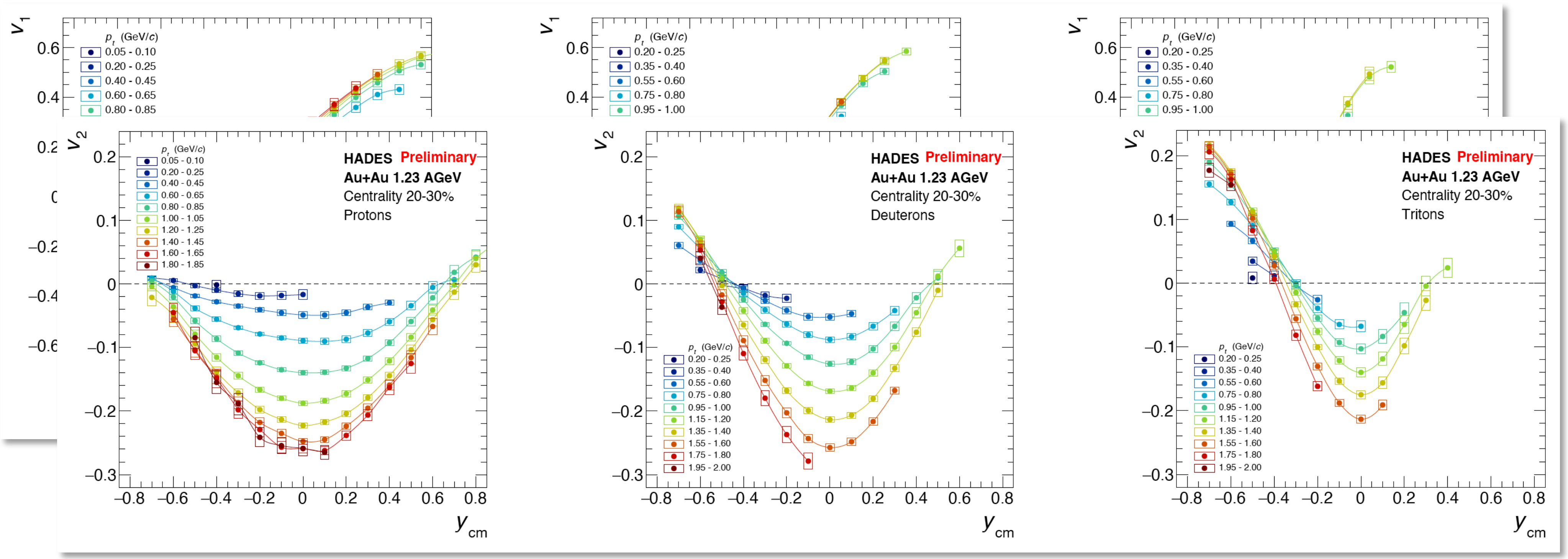

B. Kardan,
QM18

Collective Effects

Results on v_1, v_2, v_3 and v_4 for Protons, Deuterons and Tritons

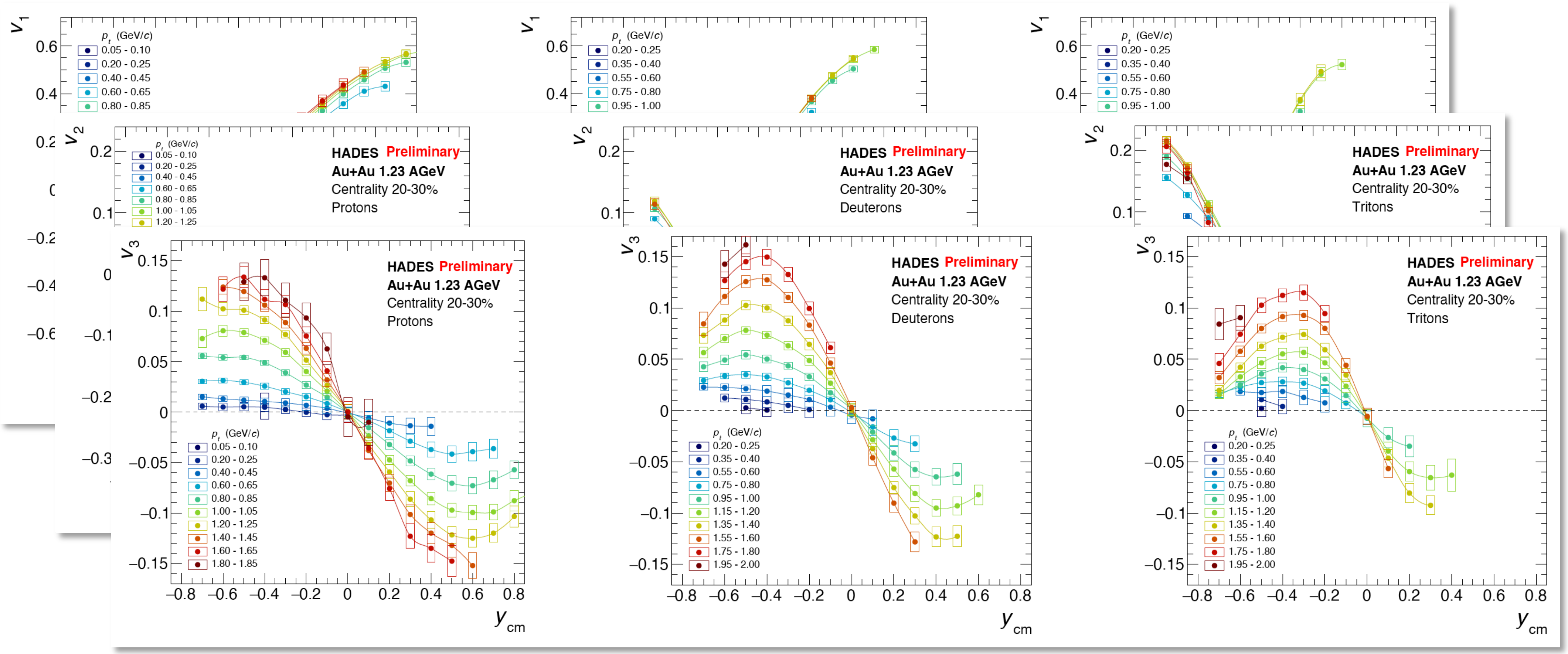

B. Kardan,
QM18

Collective Effects

Results on v_1, v_2, v_3 and v_4 for Protons, Deuterons and Tritons

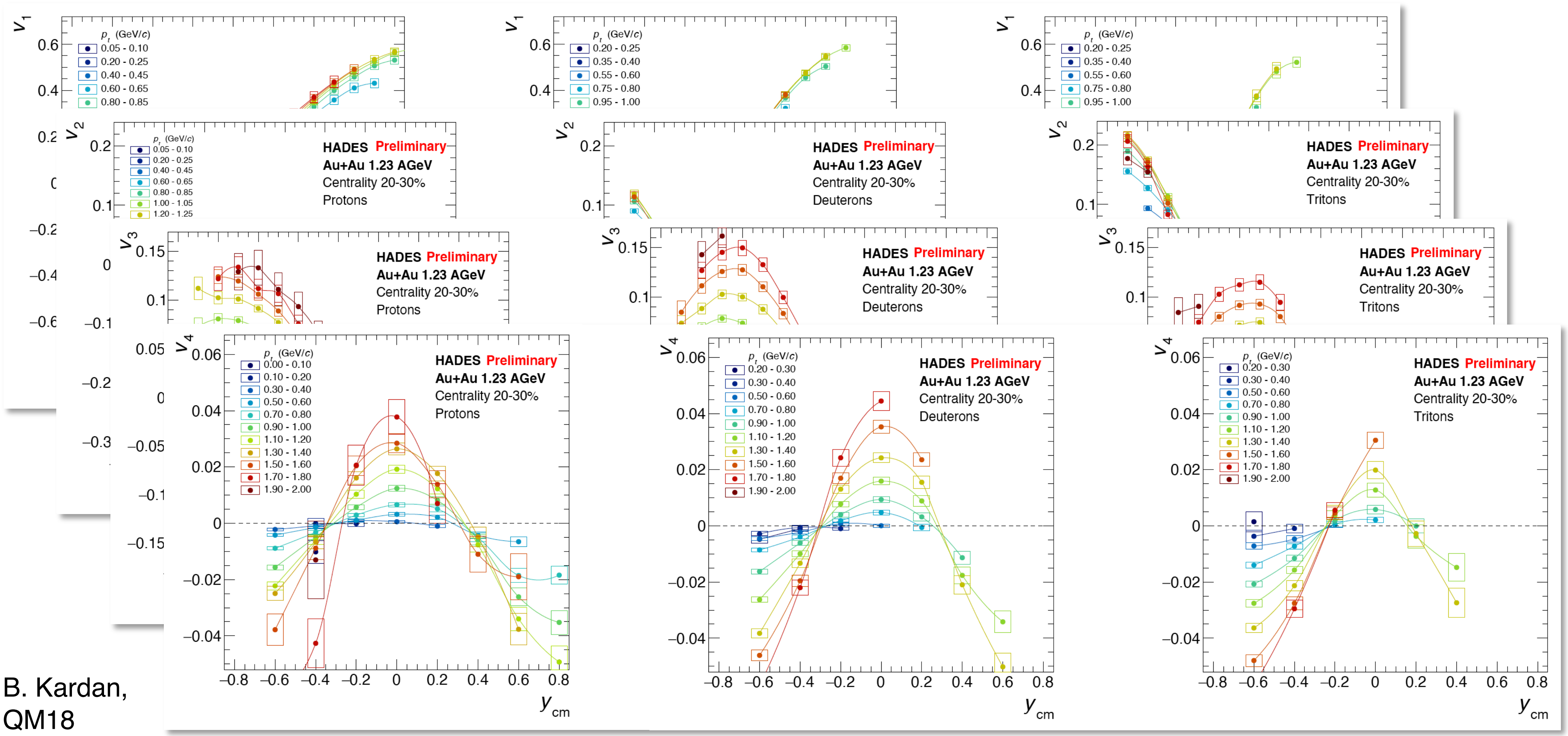

B. Kardan, QM18

Collective Effects

Relation between v_2 and v_4

Scaling properties

Prediction for ideal fluid:

$$\frac{v_4(p_t)}{v_2^2(p_t)} = \frac{1}{2}$$

P.F. Kolb, PRC **67** (2003) 031902
N. Borghini and J.-Y. Oliitrault, PLB **642** (2006) 227
C. Gombeaud and J.-Y. Ollitrault, PRC **81** (2010) 014901

Slightly higher values (~ 0.6) expected in more realistic scenario

Observed ratios for p, d and t

Independent of p_t
Close to predicted value of ~ 0.6

Hydro-like matter at HADES energies?

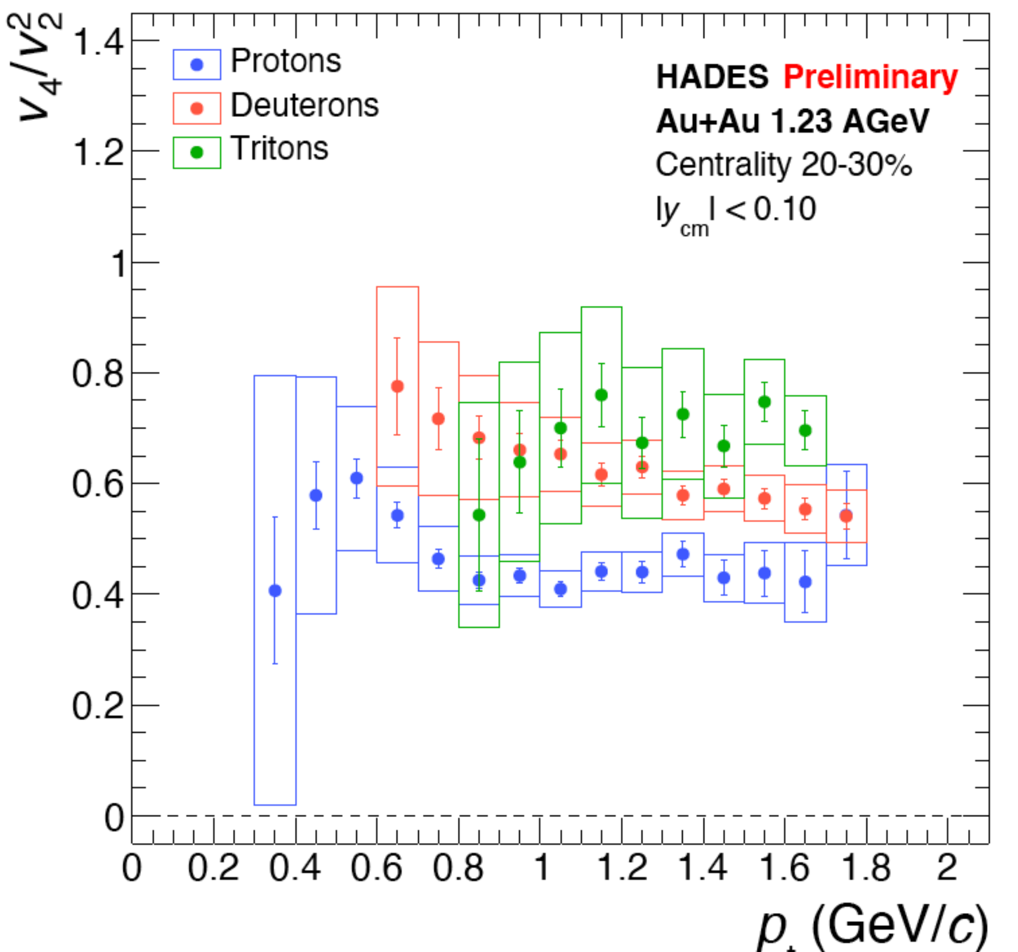

B. Kardan, SQM19

Collective Effects

Scaling Properties of v_2 at Mid-Rapidity

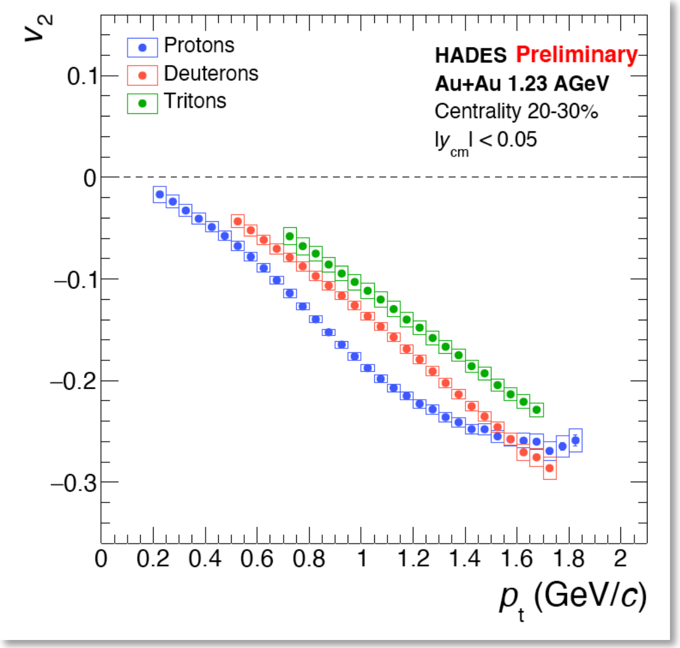

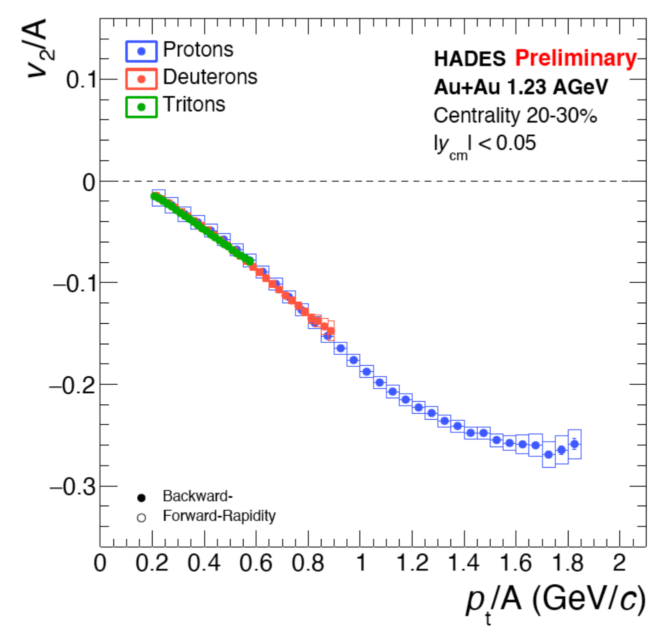

Nucleon Coalescence

Scaling of v_2 and p_t with nuclear mass number A

Works as expected in naive coalescence picture (only at mid-rapidity!)

B. Kardan, QM18
Nucl. Phys. **A982** (2019) 431

Femtoscopy
Principle

Bose-Einstein-Correlations
Pairs of identical bosons (charged pions)

Widths of correlation inversely proportional to size *R* of pion source

$$\Delta q = \frac{\hbar c}{R} \approx \frac{200}{R}\frac{GeV\,fm}{c}$$

Multi-dimensional analysis
Access to fireball evolution (radial flow)

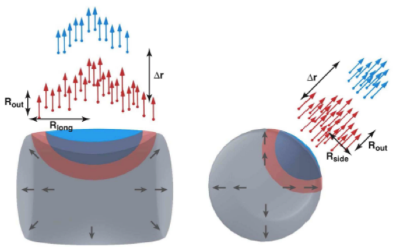

M.A. Lisa and S. Pratt, arXiv:0811.1352

Analysis relative to event plane
Access to event shapes

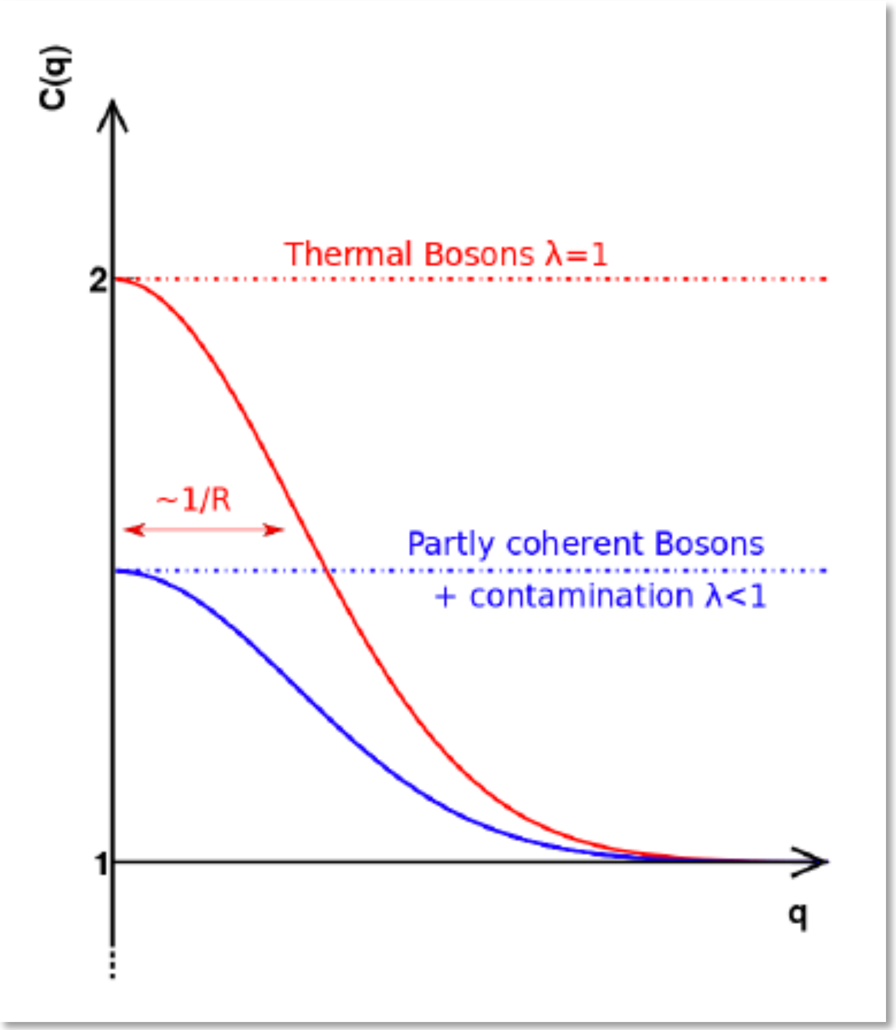

Femtoscopy
Charged-Pion Correlations

Space-time-extend of fireball
3D correlation function
Bertsch-Pratt parameterization

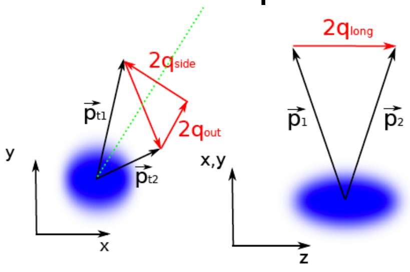

Radius parameters
Strong m_t-dependence ⟶ radial flow

1[st] observation of charge sign difference

R. Greifenhagen, QM19
Phys. Lett. **B795** (2019) 446
arXiv:1910.07885

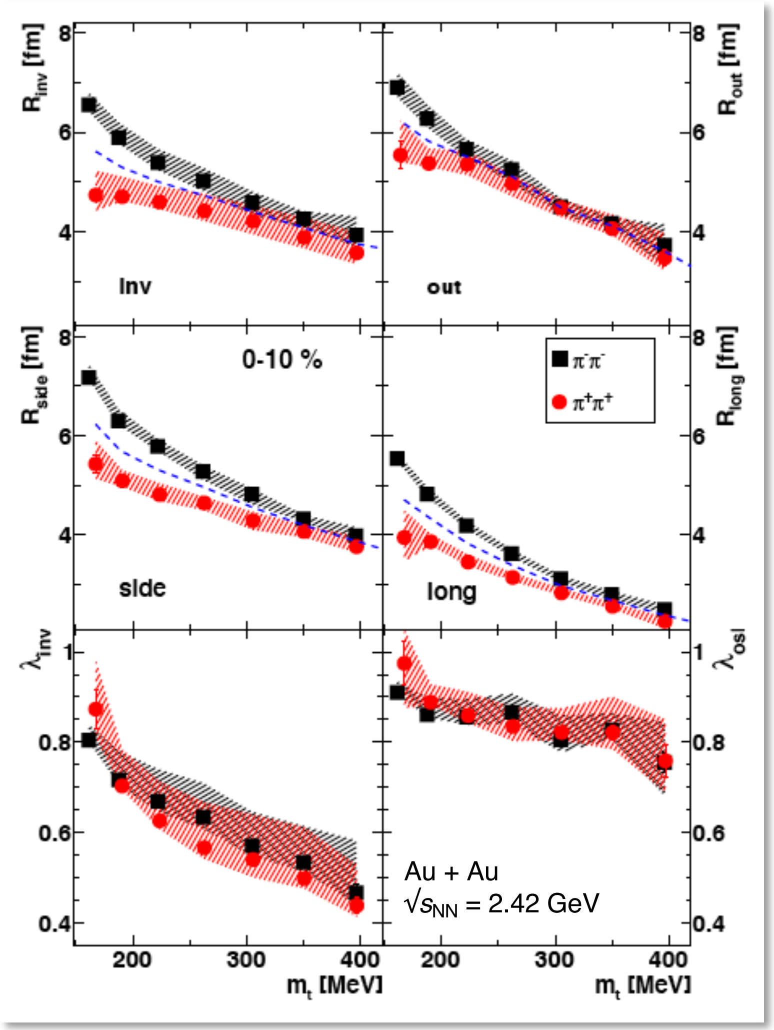

Femtoscopy

Radius Parameters

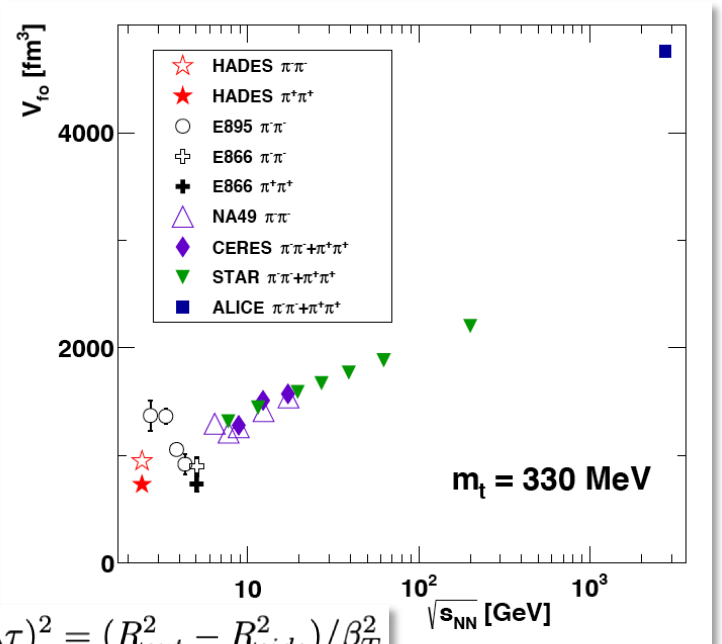

$$(\Delta\tau)^2 = (R^2_{out} - R^2_{side})/\beta^2_T$$

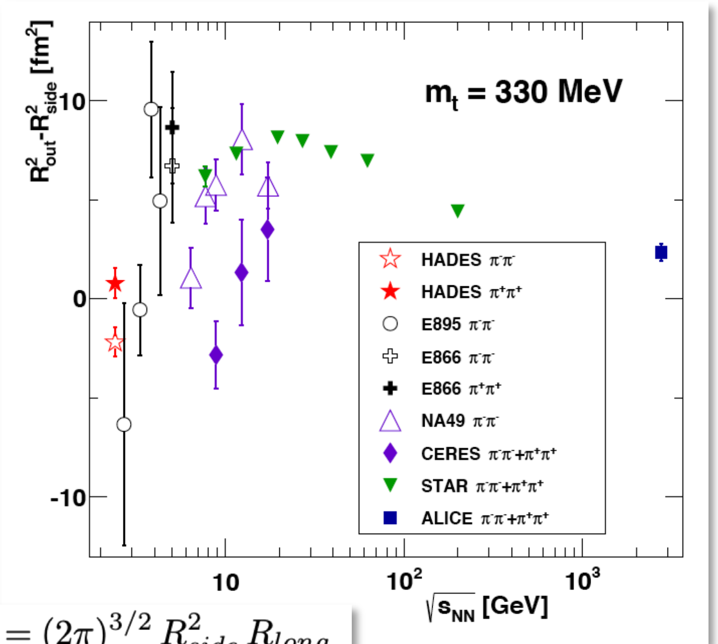

$$V_{fo} = (2\pi)^{3/2} R^2_{side} R_{long}$$

Energy dependences

Freeze-out volume: HADES result follows trend from higher energies (SPS, RHIC)
Room for structures at low energies as indicated by E895 data?

Difference between R_{out} and R_{side} close to zero (HADES), maximal for intermediate energies (top-SPS, RHIC)

R. Greifenhagen, QM19
Phys. Lett. **B795** (2019) 446
arXiv:1910.07885

Femtoscopy
Azimuthal Dependence

Fits relative to event plane
Rotation of osl-system relative to EP-system
Formulas: PLB **496** (2000) 1, PRC **57** (1998) 266
Corrected for EP-resolution

⟹ Access to event shape parameters

Eccentricity ε in xy-plane
Compare to initial participant eccentricity $\varepsilon_{\text{initial}}$ from Glauber MC

Early stage (high $p_{t,12}$):
$\varepsilon_{\text{final}} \approx \varepsilon_{\text{initial}}$

Late stage (low $p_{t,12}$):
$\varepsilon_{\text{final}} \longrightarrow 0$

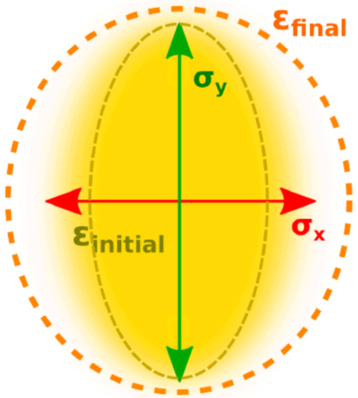

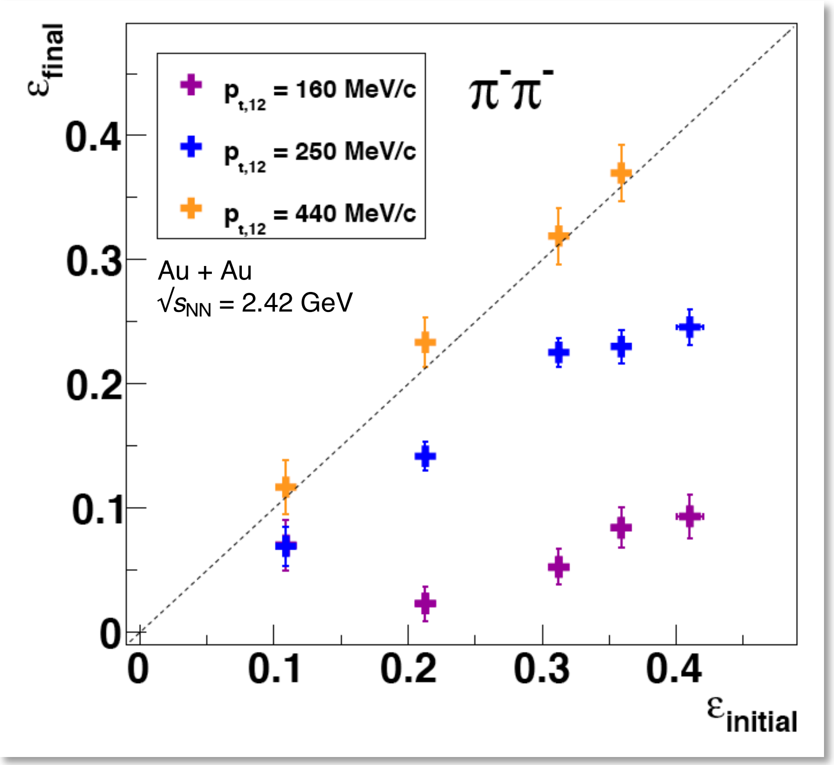

$$\epsilon_{final} = \frac{\sigma_y^2 - \sigma_x^2}{\sigma_y^2 + \sigma_x^2}$$

R. Greifenhagen, QM19
arXiv:1910.07885

Global Λ Polarization
Principle

Global polarization
Large angular momenta $|L| \sim 10^5\ \hbar$
Extreme vorticities possible ($\omega \approx 10^{21}\ s^{-1}$)

Observable via polarization of spins relative to event plane
(spin-orbit coupling, e.m.-coupling)

Observable
Weak decay: $\Lambda \longrightarrow p + \pi^-$
Proton preferentially in spin direction
$\Longrightarrow$ Polarization P_Λ:

$$P_\Lambda = \frac{8}{\pi\,\alpha_\Lambda} \frac{\langle \sin(\Psi_{EP} - \phi^*_p) \rangle}{R_{EP}}$$

Λ decay parameter: $\alpha_\Lambda = 0.643 \pm 0.013$
Ψ_{EP} = event plane angle, R_{EP} = EP-resolution
Φ^*_p = proton azimuth angle relative to EP

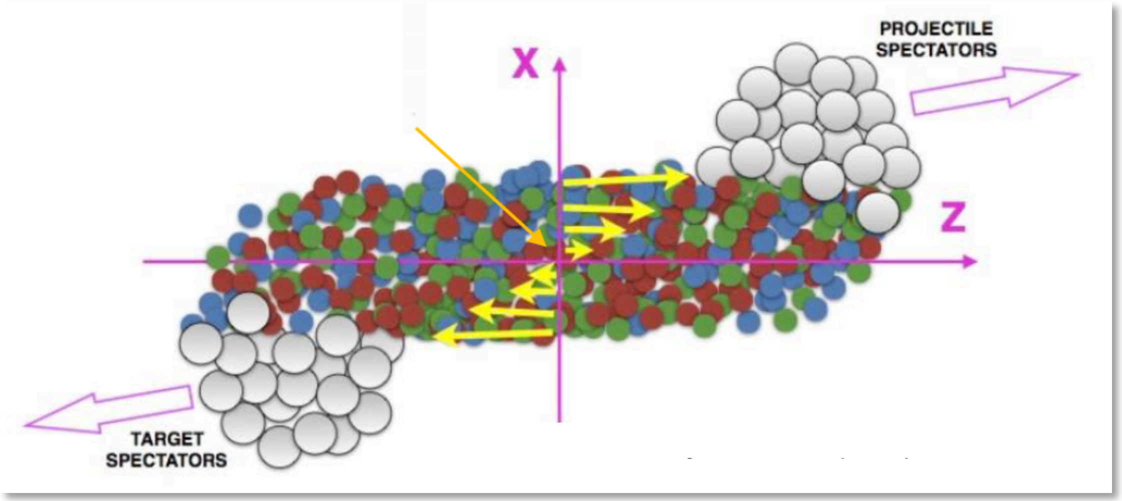

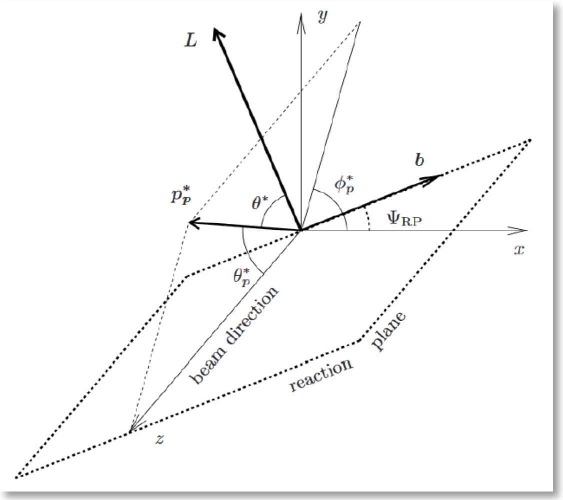

Z. Liang and X.N. Wang, PRL **94** (2005) 102301

F. Becattini et al, PRC **95** (2017) 054902

STAR Collaboration, PRC **76** (2007) 024915

F. Kornas, SQM19

Global Λ Polarization

Measurement at $\sqrt{s_{NN}}$ = 2.42 GeV

Analysis procedure

EP estimation from spectators in FW
Optimized Λ reconstruction with ANN
N_Λ – 1.9 · 10^5 (10 – 40%)

Two methods:
Invariant mass fit and EP-method

Preliminary Results

P_Λ^{EP} = (3.762 ± 0.699 (stat.)) %
P_Λ^{MINV} = (3.548 ± 0.754 (stat.)) %
Background:
P_Λ^{BG} = (3.689 ± 1.133 (stat.)) %

On-going investigations:
Systematic effects
Influence of finite detector acceptance

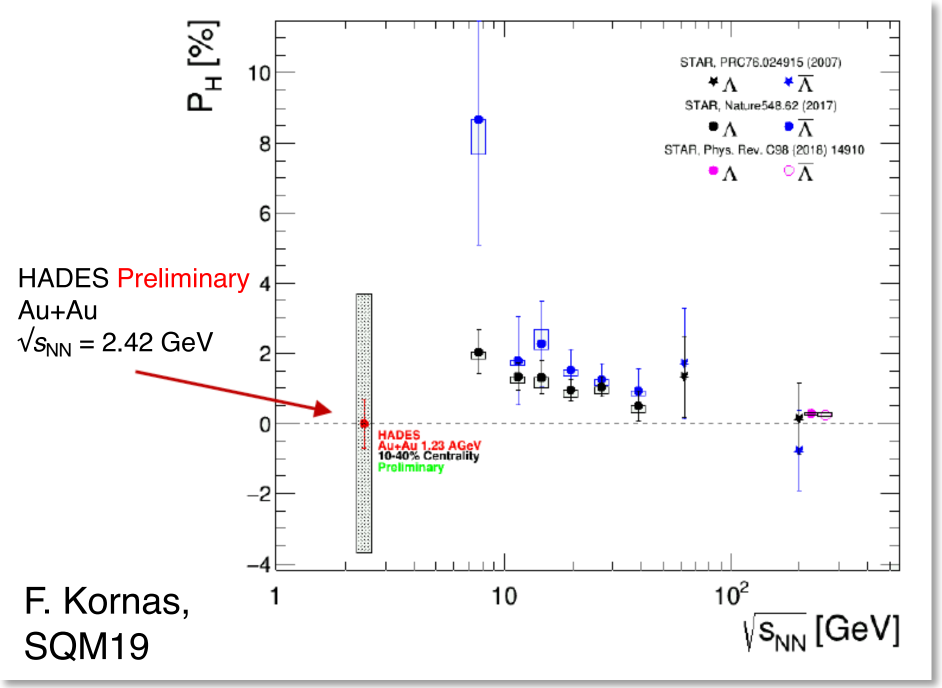

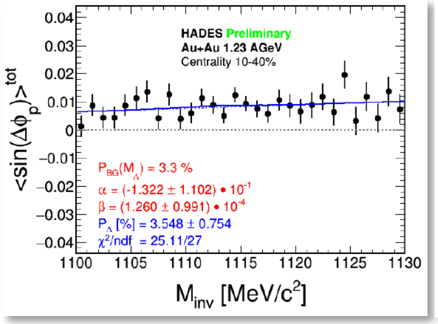

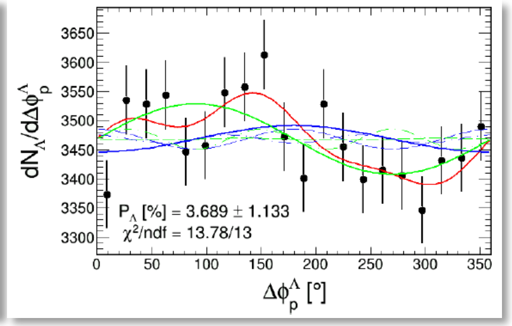

Proton Number Fluctuations
Motivation

Search for critical point
⟶ Susceptibilities diverge
⟶ Enhanced fluctuations

Fluctuations of conserved quantities (strangeness, baryon number, charge)
Higher moments should be more sensitive

Vary freeze-out conditions via energy scan

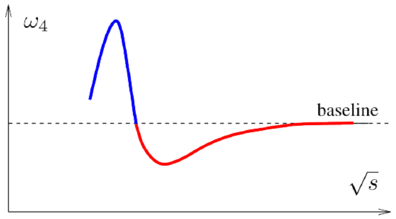

M. Stephanov

Observable
Moments of net-proton distributions (proxy for baryon number)

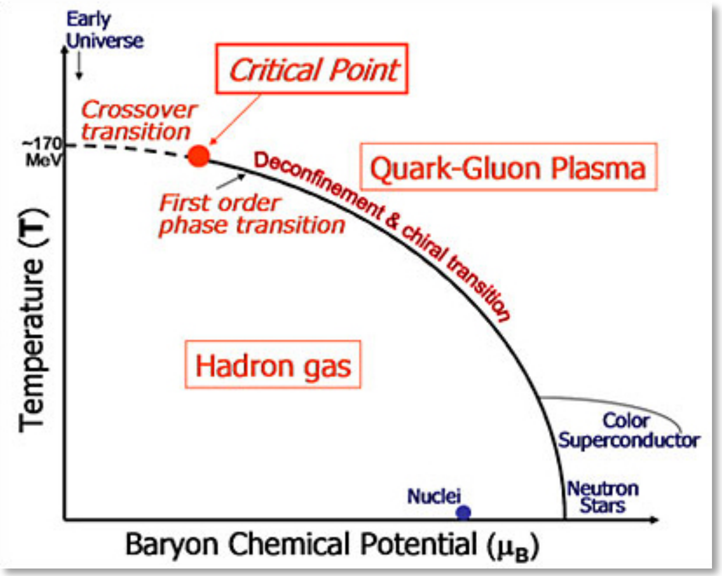

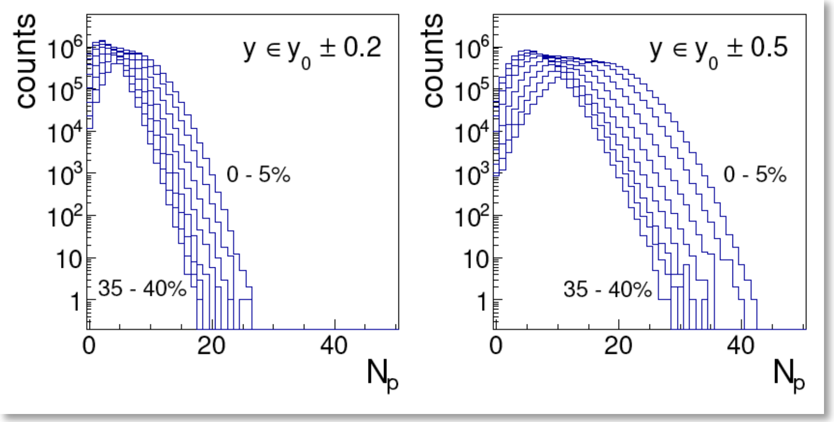

Proton Number Fluctuations

Corrections

Observable (HADES)

Moments of proton multiplicity distributions
Centrality selection with Forward Wall (5%)

Efficiency correction

Track density dependent efficiency
Evaluated via three different methods

Binomial E-by-E: A. Bzdak and V. Koch, PRC **86** (2012) 044904
S. He and X. Luo, Chin. Phys. **C42** (2018) 104001
Unfolding: P. Garg et al., J. Phys. G **40** (2013) 055103
Moment expansion: T. Nonaka et al., NIM **A906** (2018) 10

Volume corrections

Extension of assumption of constant reduced cumulants $\kappa_n(V) = K_n/V = const.$

V. Skokov et al., PRC **88** (2013) 034911
P. Braun-Munzinger et al., NPA **960** (2017) 114

Here: 2nd-order approach:

$$\kappa_n(V) = \kappa_n + \kappa_n'(V - \langle V\rangle) + \kappa_n''(V - \langle V\rangle)^2$$

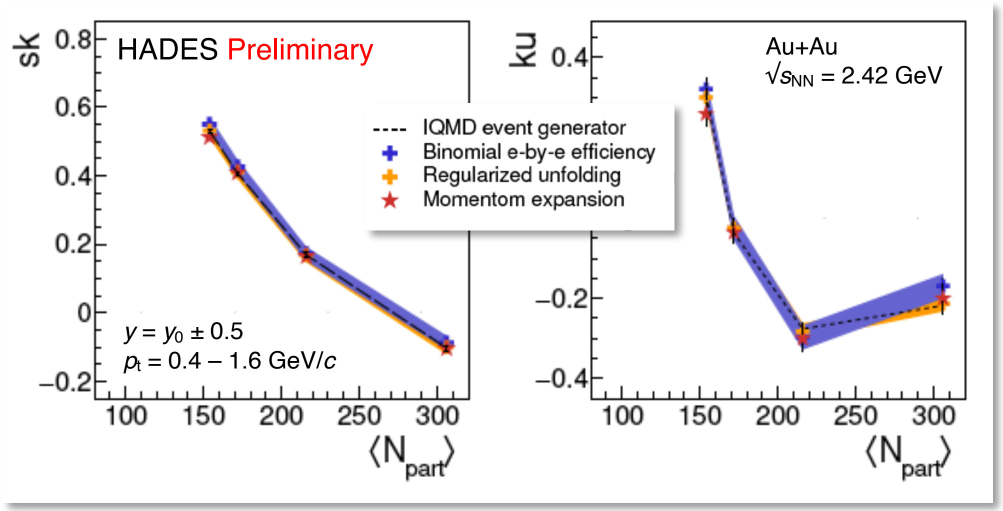

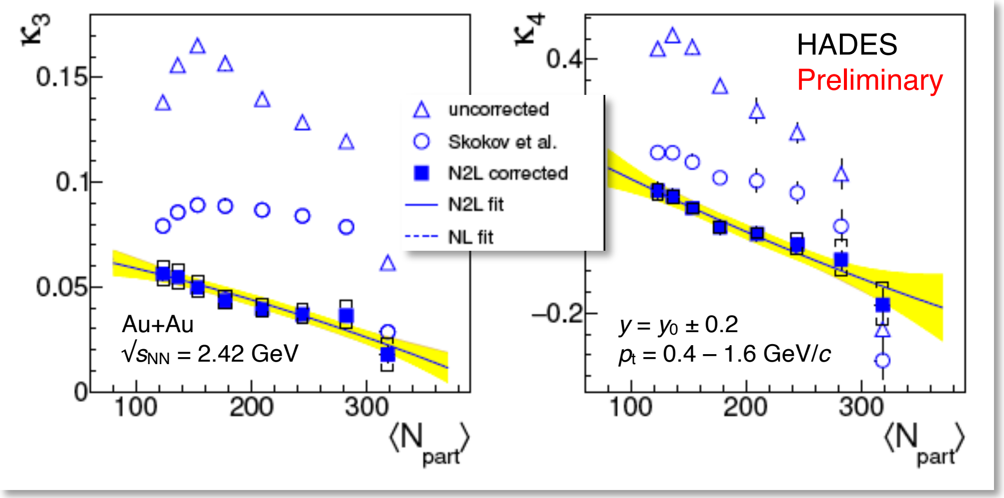

Proton Number Fluctuations

Energy Dependence of Scaled Cumulants

Extension of STAR-BES results

Skewness ($Sk \cdot \sigma$): smooth trend
Kurtosis ($Ku \cdot \sigma^2$): change of sign (0-5%)

Contribution from spectators

Fluctuation sources: fireball ↔ spectators
Relative admixture energy dependent!

⟹ Two rapidity intervals shown:
$y_0 \pm 0.2$ and $y_0 \pm 0.4$ (STAR: $y_0 \pm 0.5$)

Outlook

Include bound protons (d, t, He)
Ag+Ag data

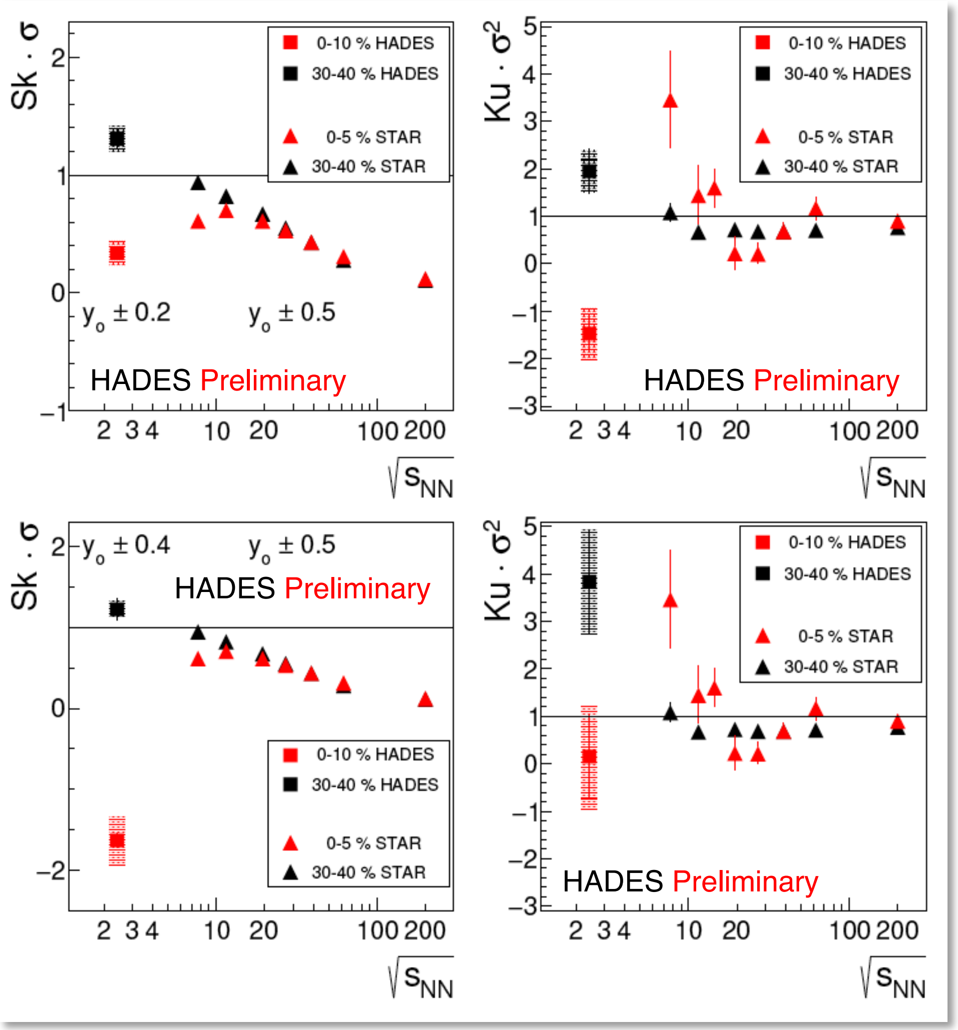

FAIR Phase-0

Ag+Ag at $\sqrt{s_{NN}}$ = 2.6 GeV

New data set from March 2019

~ 15 billion events collected

Upgraded setup

New RICH photon detector (same MAPTs as for CBM)

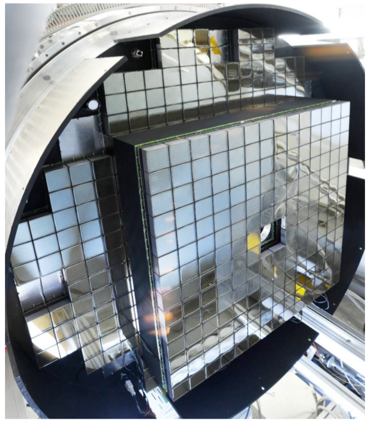

Electromagnetic calorimeter
⟹ Poster by P. Chudoba
⟹ Talk by A. Rost

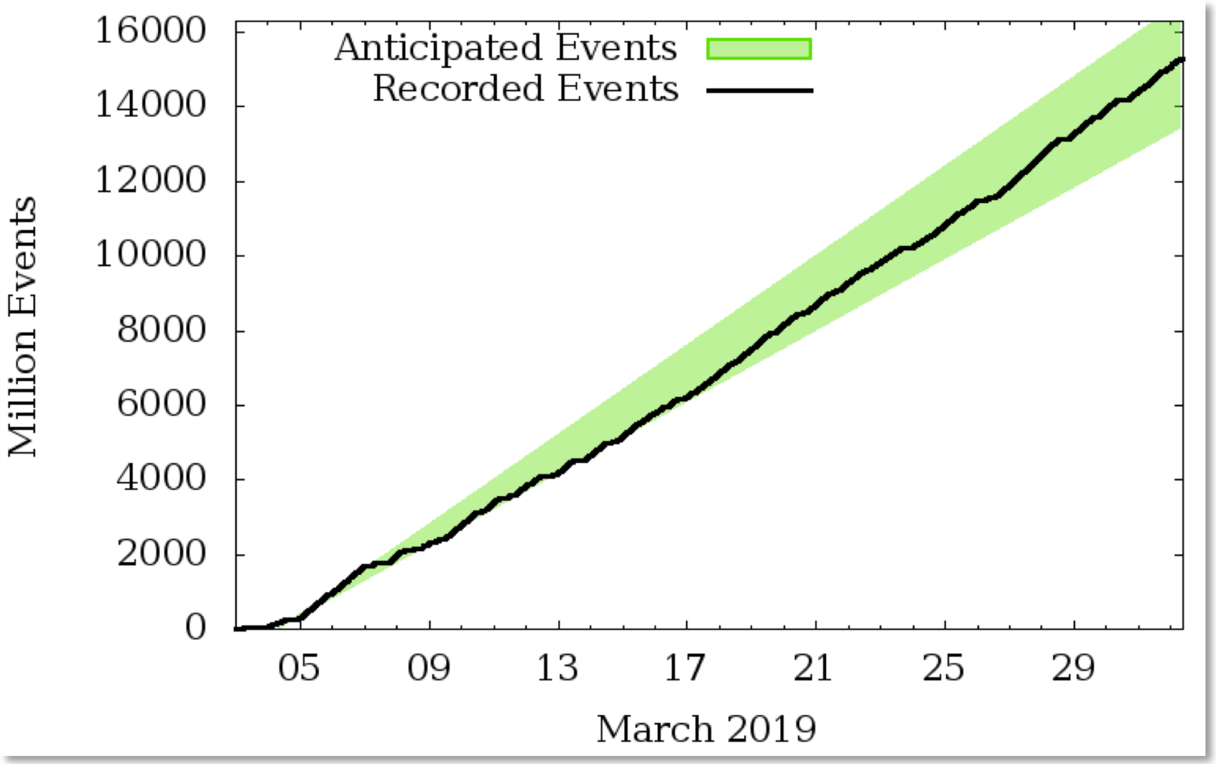

FAIR Phase-0

Ag+Ag at $\sqrt{s_{NN}}$ = 2.6 GeV

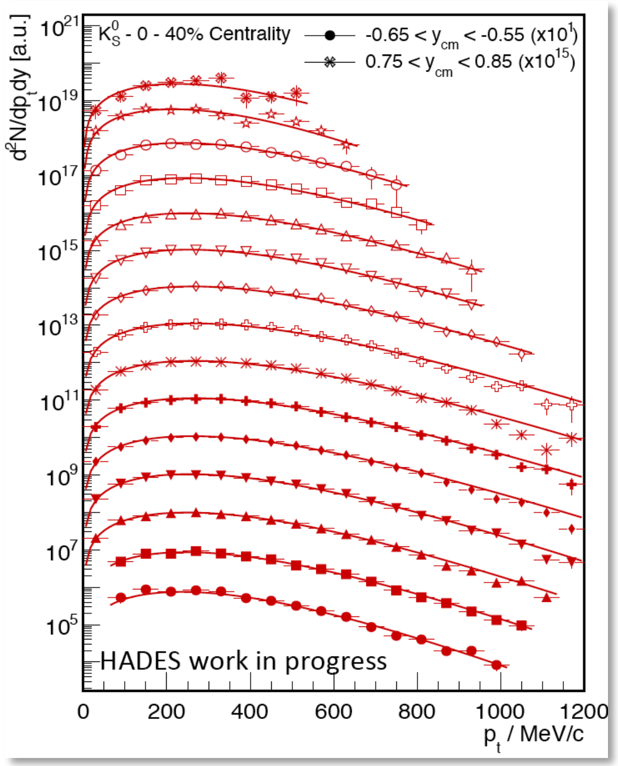

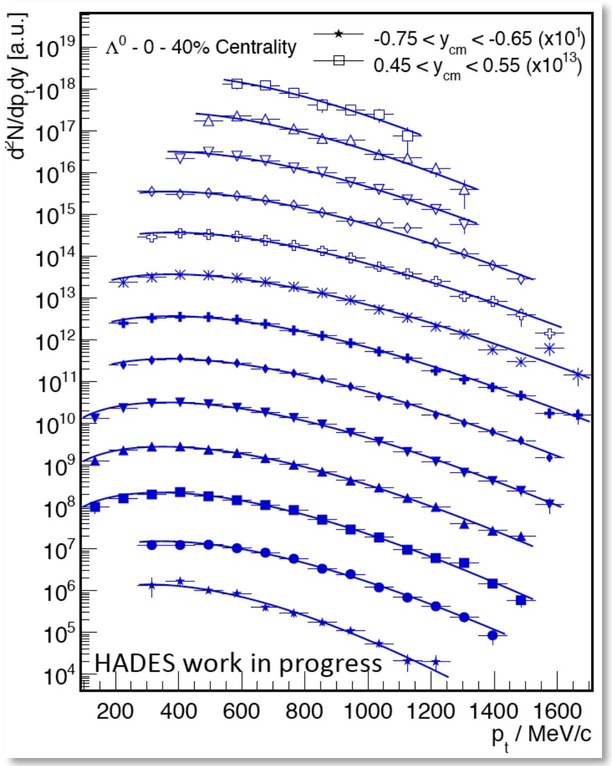

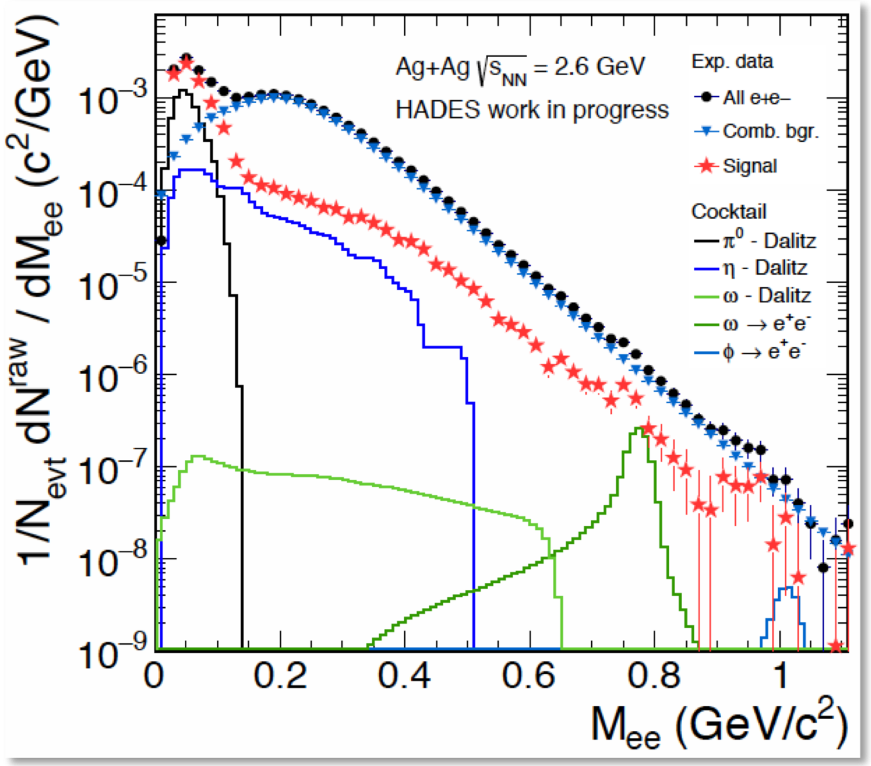

First glimpse into new data set

K^0_s and Λ spectra at the NN-threshold

1st Dilepton spectrum

Conclusions

HADES

“Thermalized” system at high baryon densities

Particle yields at freeze-out
Flow properties
Thermal di-electron excess

Low energy point in excitation functions

Femtoscopy radii
Global Λ polarization
Proton fluctuations

In-medium effects in cold nuclear matter

Evidence for kaon and ϕ absorption

Strong scientific program for FAIR Phase-0

Ag+Ag at $\sqrt{s_{NN}}$ = 2.6 GeV
π + A Program at SIS18

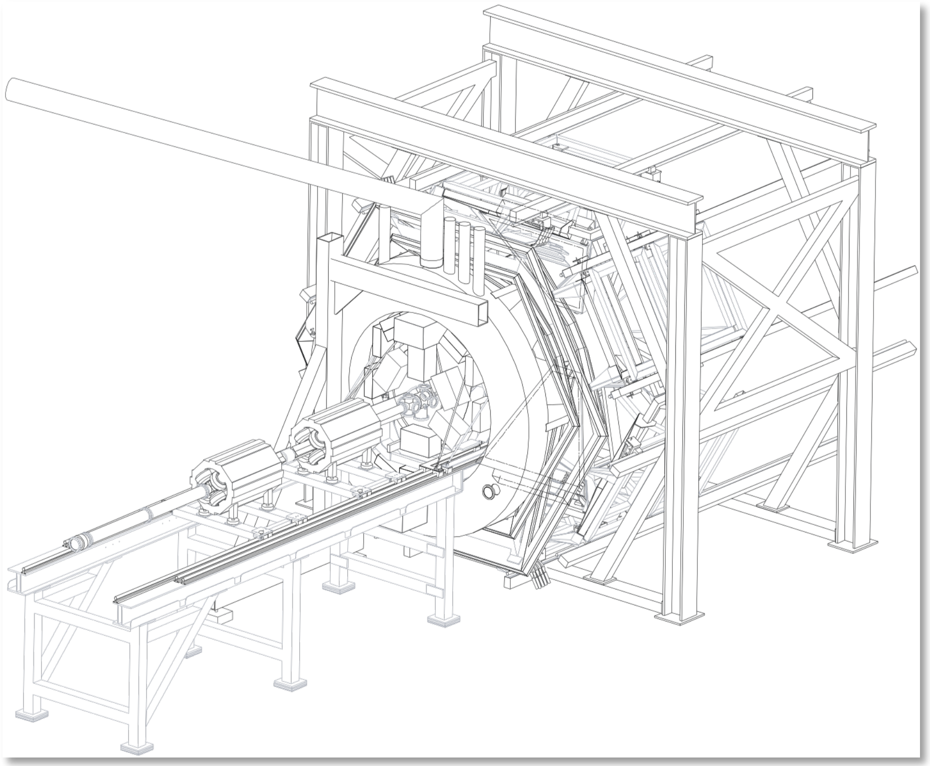


WYDZIAŁ FIZYKI ASTRONOMII I INFORMATYKI STOSOWANEJ
Many Thanks!
The HADES Collaboration

BACKUP

Particle Production

Protons, Deuterons and Tritons

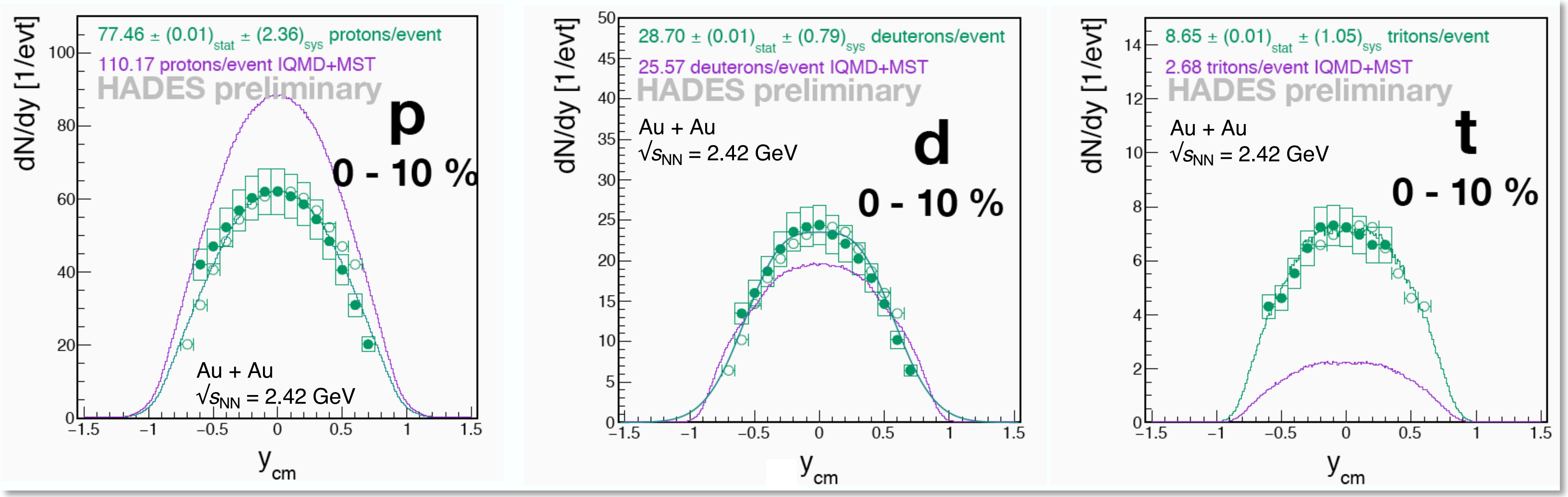

Comparison to simple coalescence approach

Transport model + clustering afterburner (IQMD + MST*, $r = 5$ fm in pos. space, $t < 140$ fm/c)
Unable to reproduce triton data

Comparisons to more involved calculations on-going

M. Szala, SQM19

*Thanks to Y. Leifels

Particle Production

Particle Yields ⟶ Chemical Freeze-Out

Fit with THERMAL-FIST

Freeze-Out parameters (T_{chem}, μ_B) follow universal freeze-out curve

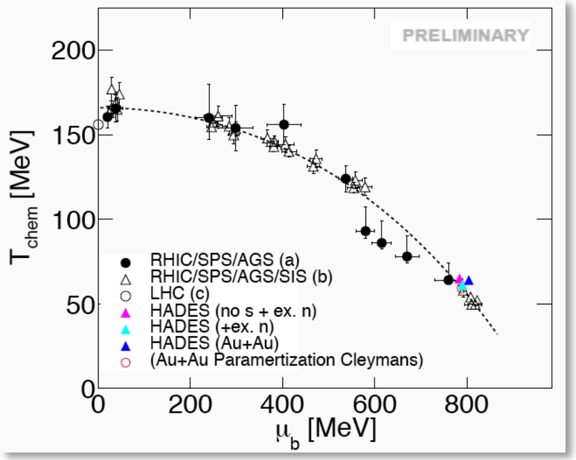

Freeze-out points
J. Cleymans, H. Oeschler and K. Redlich, Phys. Rev. **C59** (1999)
R. Averbeck, R. Holzmann, V. Metag and R.S. Simon, Phys. Rev. **C67** (2003)

Relatively high χ^2 for full hadron spectrum

Inclusion of excited nuclei states helps
Add. exclusion of strangeness ⇒ small χ^2
(see backup slides)

Thermal Fist: V. Vovchenko H. Stoecker, Comput. Phys. Commun. 244 (2019) 295.

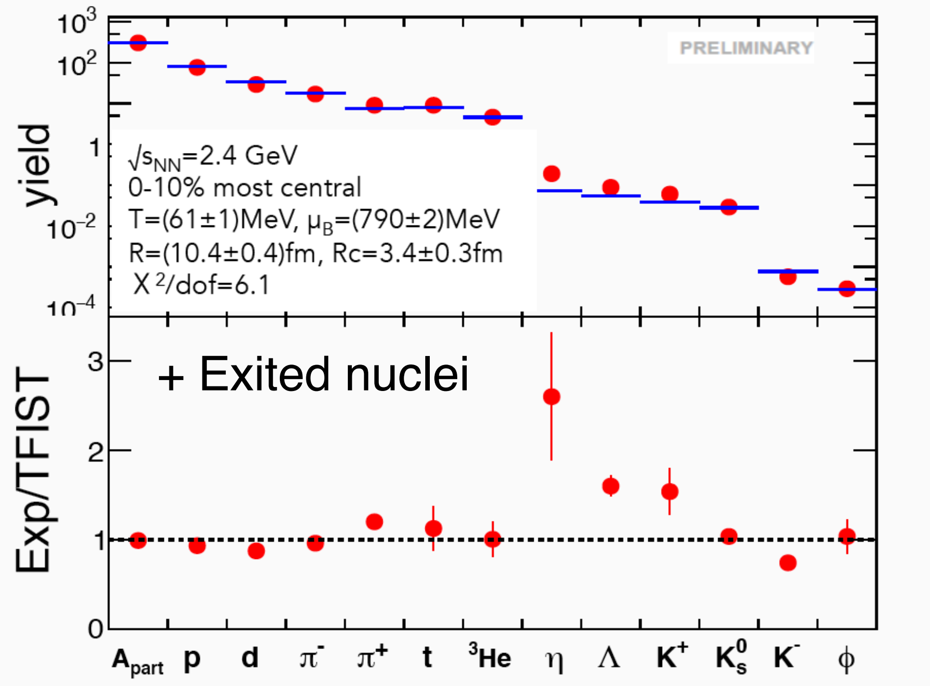

M. Lorenz,
EMMI-Workshop on Anti-matter, hyper-matter and exotica

Particle Production

Particle Yields ⟶ Chemical Freeze-Out

Fit with THERMAL-FIST

Freeze-Out parameters (T_{chem}, μ_B) follow universal freeze-out curve

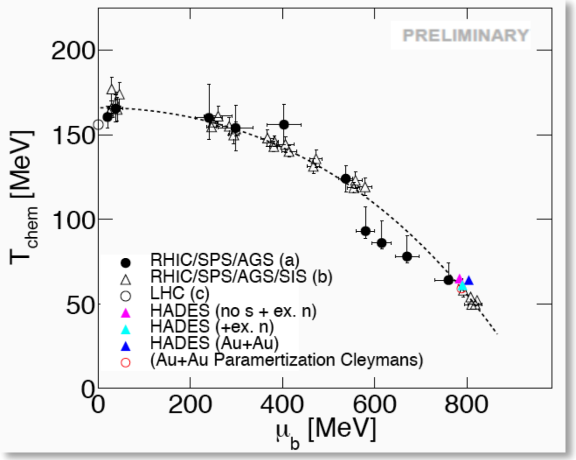

Freeze-out points
J. Cleymans, H. Oeschler and K. Redlich, Phys. Rev. **C59** (1999)
R. Averbeck, R. Holzmann, V. Metag and R.S. Simon, Phys. Rev. **C67** (2003)

Relatively high χ^2 for full hadron spectrum

Inclusion of excited nuclei states helps
Add. exclusion of strangeness ⇒ small χ^2
(see backup slides)

Thermal Fist: V. Vovchenko H. Stoecker, Comput. Phys. Commun. 244 (2019) 295.

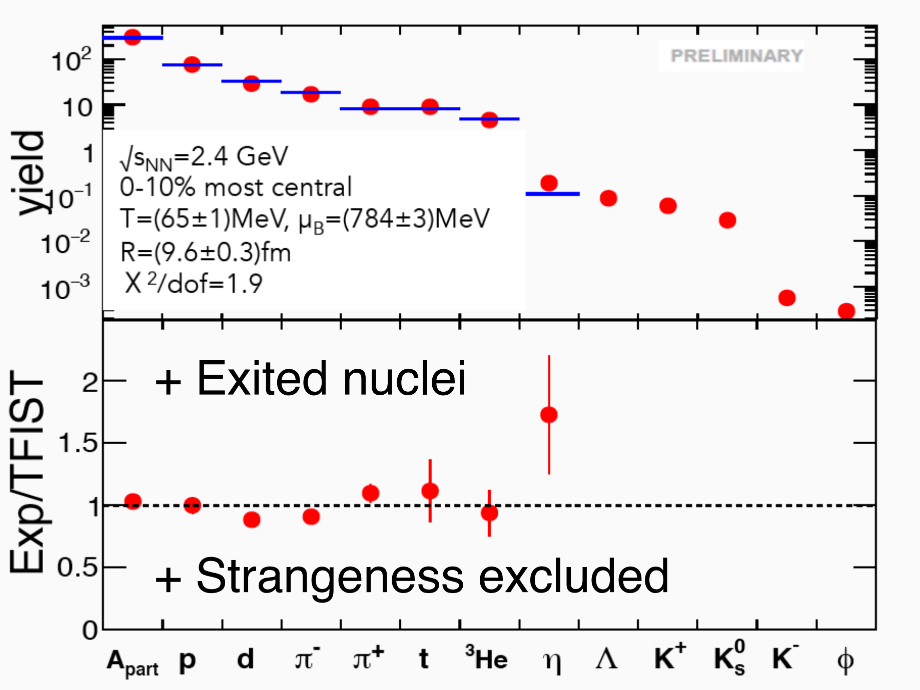

M. Lorenz,
EMMI-Workshop on Anti-matter, hyper-matter and exotica

Femtoscopy
Azimuthal Dependence

Fits relative to event plane

Rotation of osl-system relative to EP-system

Formulas: PLB **496** (2000) 1, PRC **57** (1998) 266

Corrected for EP-resolution

⟹ Access to event shape parameters

Tilt angle θ_s in xz-plane

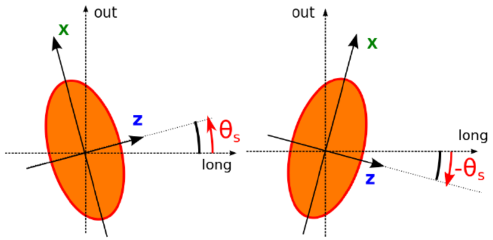

$|\theta_s|$ tends to decrease with increasing $p_{t,12}$

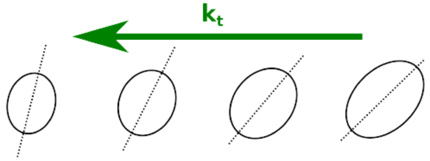

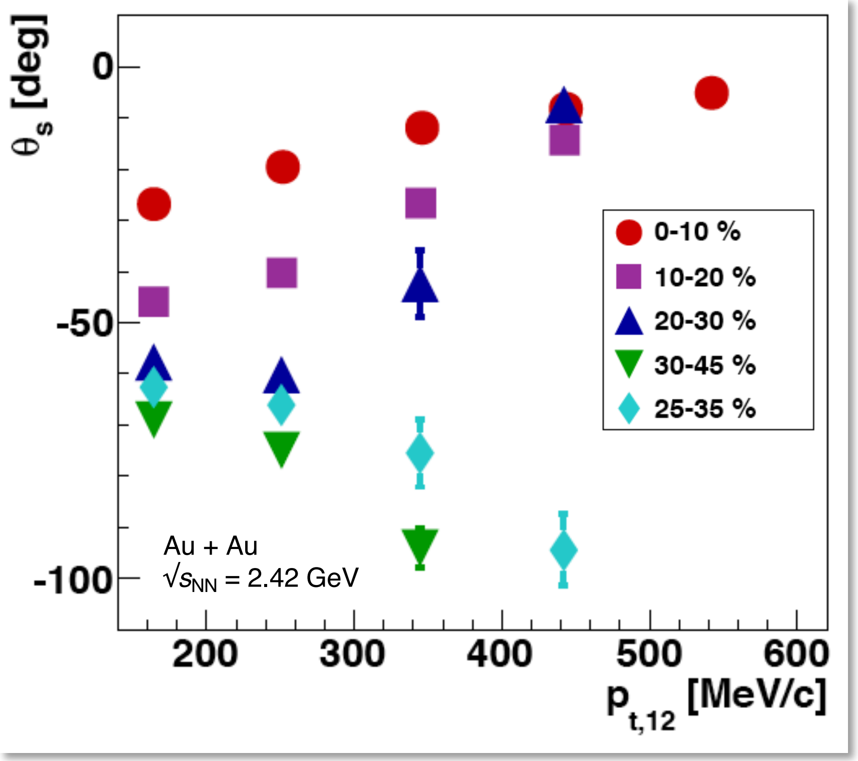

R. Greifenhagen, QM19
arXiv:1910.07885

Collective Effects

Directed and Elliptic Flow of Kaons

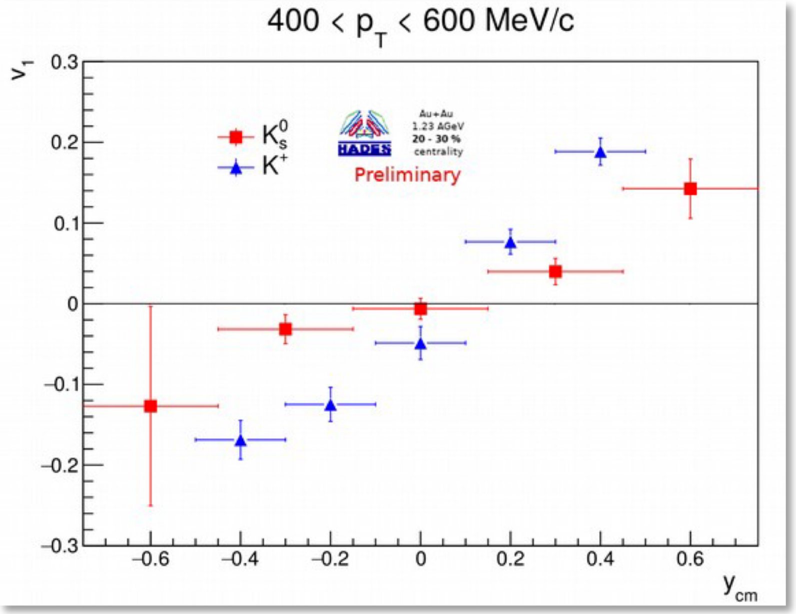

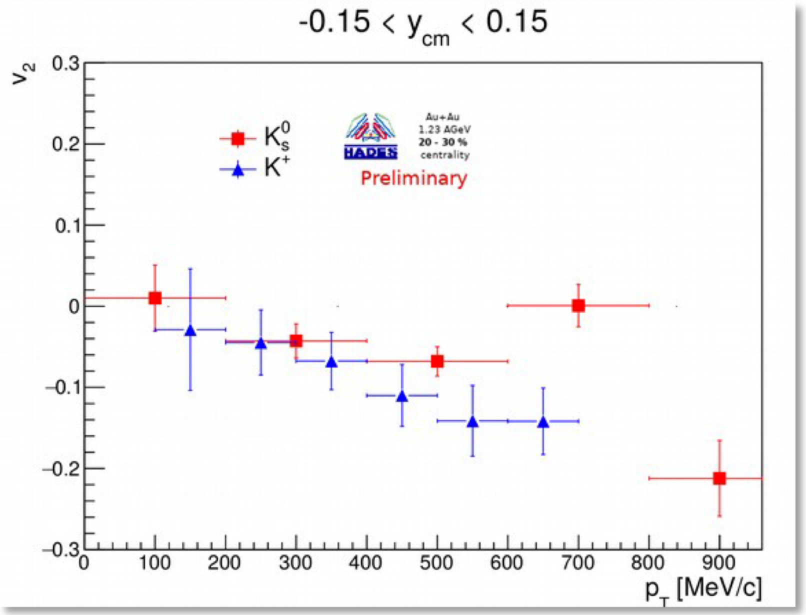

Collective Effects

Scaling Properties of v_4 at Mid-Rapidity

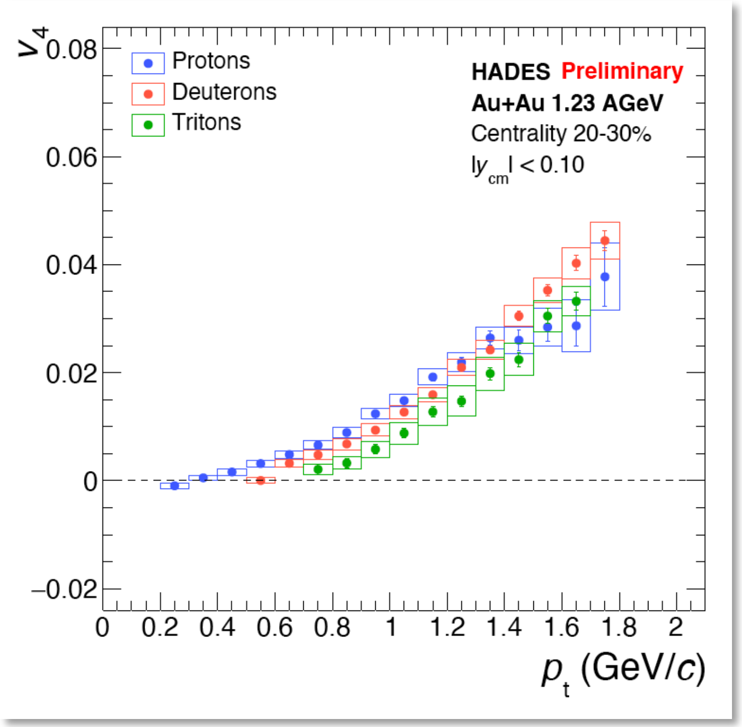

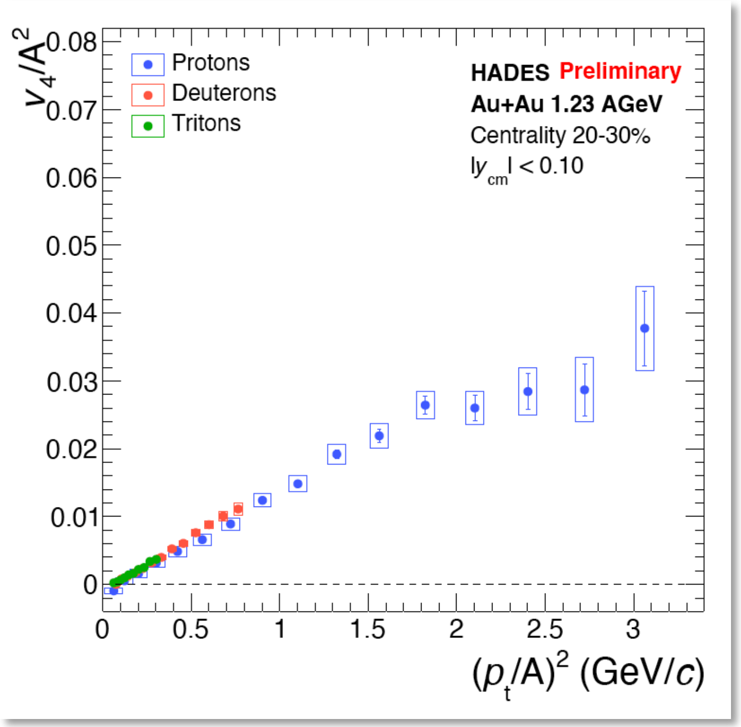

Femtoscopy
Energy Dependence of Radius Parameters

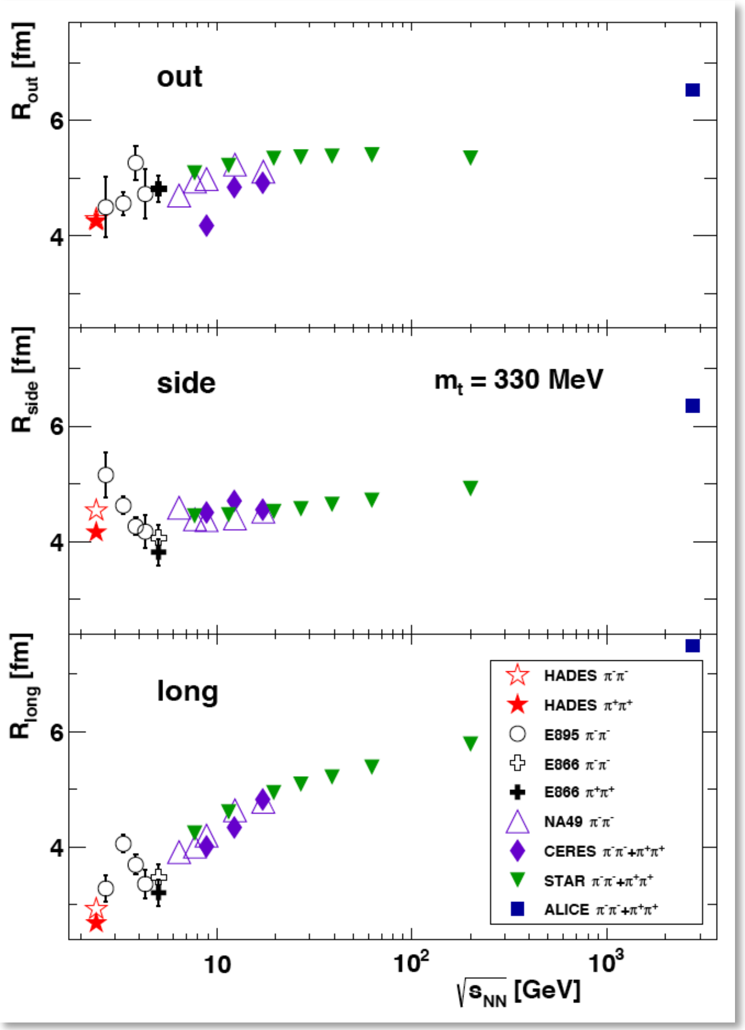

Femtoscopy

Radius Parameters

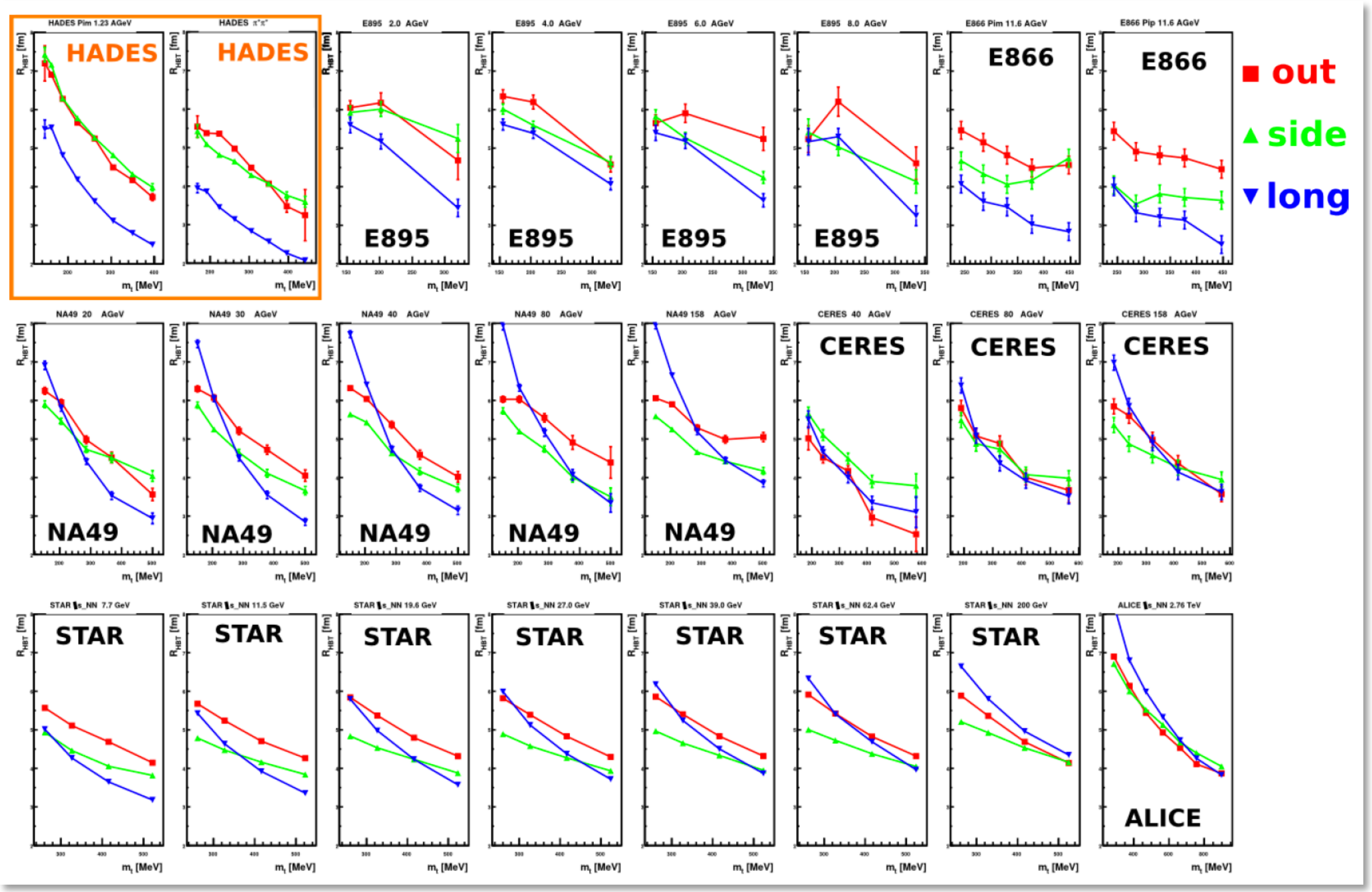

Particle Production

Pions

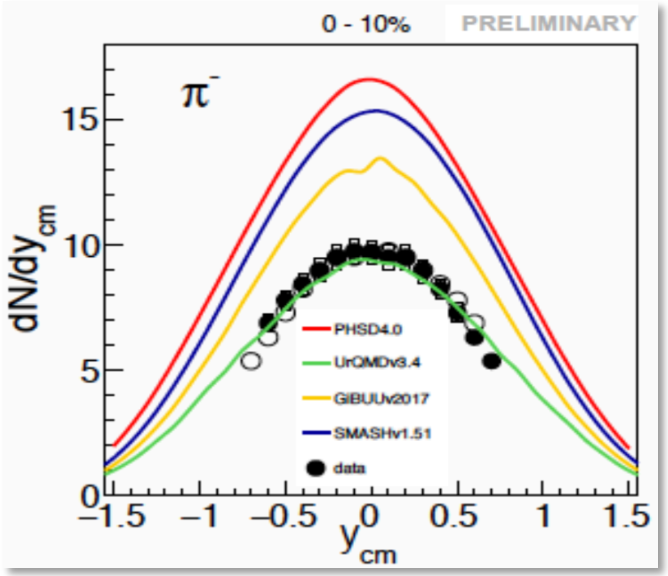

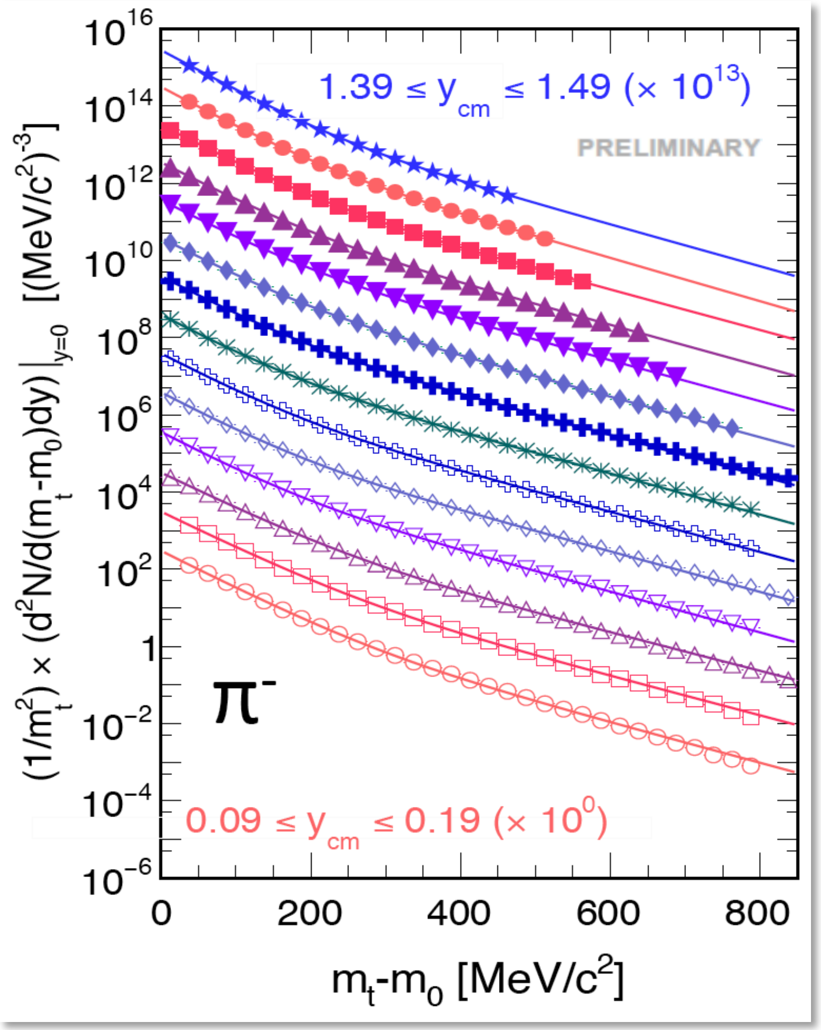

Particle Production
Pions

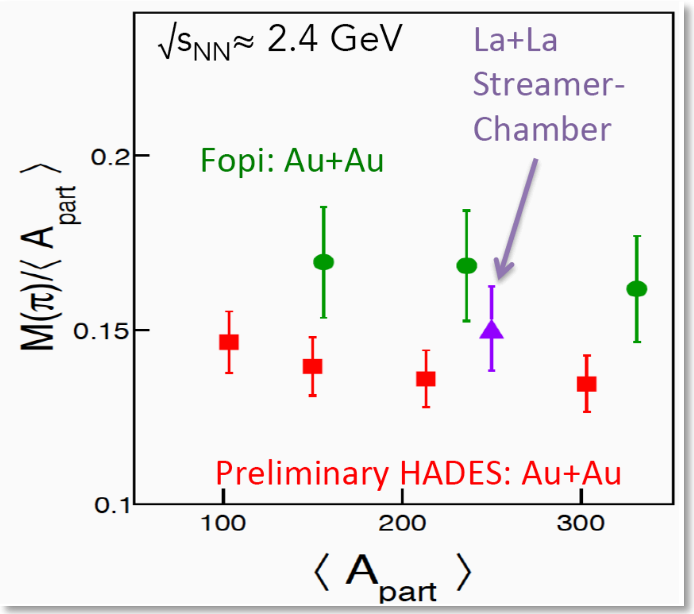

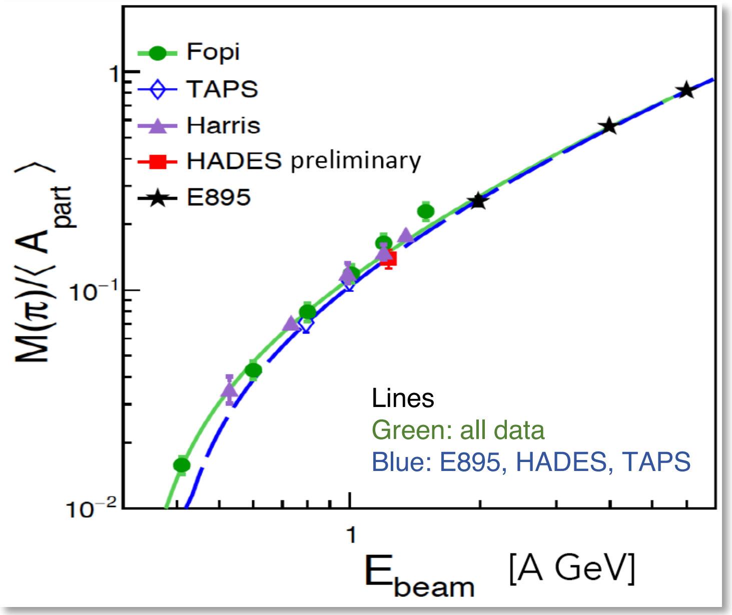

J.W. Harris et al., Phys. Rev. Lett. **58** (1987) 463
R. Averbeck et al. [TAPS], Phys. Rev. **C67** (2003) 024903
J.L. Klay et al. [E895], Phys. Rev. **C68** (2003) 054905
W. Reisdorf et al. [FOPI], Nucl. Phys. **A781** (2007) 459

Proton Number Fluctuations

Efficiency Correction

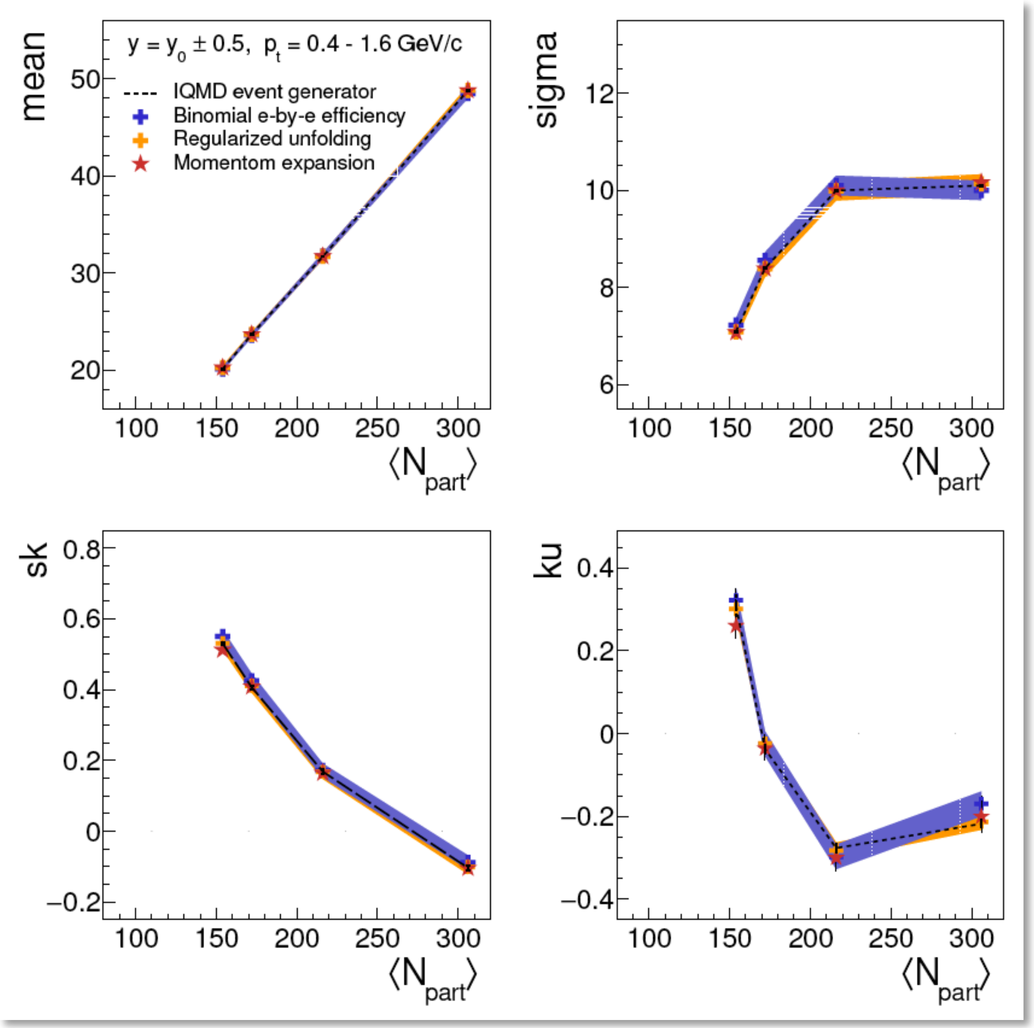

Proton Number Fluctuations

NNLO Volume Corrections

$$
\begin{aligned}
\tilde{\kappa}_1 &= \kappa_1 + \upsilon_2 \kappa'_1 \,, \\
\tilde{\kappa}_2 &= \kappa_2 + \kappa_1^2 \upsilon_2 + \kappa'_2 \upsilon_2 + 2\kappa_1 \kappa'_1 V_2 + 2\kappa_1 \kappa'_1 \upsilon_3 + 2\kappa_1'^2 \upsilon_2 V_2 + \kappa_1'^2 V_1 V_2 + 2\kappa_1'^2 V_3 + \kappa_1'^2 \upsilon_4 \,, \\
\tilde{\kappa}_3 &= \kappa_3 + \kappa_1^3 \upsilon_3 + 3\kappa_1 \kappa_2 \upsilon_2 + 3(\kappa_1 \kappa'_2 + \kappa'_1 \kappa_2)\upsilon_3 + 6\kappa'_1(\kappa_1^2 + \kappa'_2)\upsilon_2 V_2 + 3\kappa'_1(\kappa_1^2 + 2\kappa'_2) V_3 \\
&\quad + 3\kappa'_1(\kappa_1^2 + \kappa'_2)\upsilon_4 + 12\kappa_1 \kappa_1'^2 V_2^2 + 3\kappa_1 \kappa_1'^2 V_1 V_3 + 24\kappa_1 \kappa_1'^2 \upsilon_2 V_3 + 6\kappa_1 \kappa_1'^2 V_4 + 3\kappa_1 \kappa_1'^2 \upsilon_5 \\
&\quad + 3(\kappa_1 \kappa'_2 + \kappa'_1 \kappa_2) V_2 + 8\kappa_1'^3 \upsilon_2 V_2^2 + 6\kappa_1'^3 V_1 V_2^2 + 10\kappa_1'^3 \upsilon_3 V_3 + \kappa_1'^3 V_1^2 V_3 + 24 V_2 V_3 \kappa_1'^3 \\
&\quad + 3\kappa_1'^3 V_1 V_4 + 12\kappa_1'^3 \upsilon_2 V_4 + 3\kappa_1'^3 V_5 + \kappa_1'^3 \upsilon_6 + 3\kappa'_1 \kappa'_2 V_1 V_2 + \kappa'_3 \upsilon_2 \,, \\
\tilde{\kappa}_4 &= \kappa_4 + \kappa_1^4 \upsilon_4 + 6\kappa_1^2 \kappa_2 \upsilon_3 + (4\kappa_1 \kappa_3 + 3\kappa_2^2)\upsilon_2 + 24(\kappa_1^3 \kappa'_1 + 4\kappa_1 \kappa'_1 \kappa'_2 + 2\kappa_1'^2 \kappa_2)\upsilon_2 V_3 \\
&\quad + 4(\kappa_1^3 \kappa'_1 + 6\kappa_1 \kappa'_1 \kappa'_2 + 3\kappa_1'^2 \kappa_2) V_4 + 2(2\kappa_1^3 \kappa'_1 + 6\kappa_1 \kappa'_1 \kappa'_2 + 3\kappa_1'^2 \kappa_2)\upsilon_5 \\
&\quad + 48(\kappa_1^2 \kappa_1'^2 + \kappa_1'^2 \kappa'_2)\upsilon_2 V_2^2 + 12(4\kappa_1^2 \kappa_1'^2 + 5\kappa_1'^2 \kappa'_2)\upsilon_3 V_3 + 72(\kappa_1^2 \kappa_1'^2 + 2\kappa_1'^2 \kappa'_2) V_2 V_3 \\
&\quad + 6(\kappa_1^2 \kappa_1'^2 + 3\kappa_1'^2 \kappa'_2) V_1 V_4 + 72(\kappa_1^2 \kappa_1'^2 + \kappa_1'^2 \kappa'_2)\upsilon_2 V_4 + 6(2\kappa_1^2 \kappa_1'^2 + 3\kappa_1'^2 \kappa'_2) V_5 \\
&\quad + 6(\kappa_1^2 \kappa_1'^2 + \kappa_1'^2 \kappa'_2)\upsilon_6 + 2(6\kappa_1^2 \kappa'_2 + 12\kappa_1 \kappa'_1 \kappa_2 + 4\kappa'_1 \kappa'_3 + 3\kappa_2'^2)\upsilon_2 V_2 \\
&\quad + 2(3\kappa_1^2 \kappa'_2 + 6\kappa_1 \kappa'_1 \kappa_2 + 4\kappa'_1 \kappa'_3 + 3\kappa_2'^2) V_3 + 2(3\kappa_1^2 \kappa_2 + 2\kappa_1 \kappa'_3 + 2\kappa'_1 \kappa_3 + 3\kappa_2 \kappa'_2)\upsilon_3 \\
&\quad + (6\kappa_1^2 \kappa'_2 + 12\kappa_1 \kappa'_1 \kappa_2 + 4\kappa'_1 \kappa'_3 + 3\kappa_2'^2)\upsilon_4 + 96\kappa_1 \kappa_1'^3 V_2^3 + 96\kappa_1 \kappa_1'^3 V_3^2 + 288\kappa_1 \kappa_1'^3 \upsilon_3 V_2^2 \\
&\quad + 72\kappa_1 \kappa_1'^3 V_1 V_2 V_3 + 4\kappa_1 \kappa_1'^3 V_1^2 V_4 + 144\kappa_1 \kappa_1'^3 V_2 V_4 + 128\kappa_1 \kappa_1'^3 \upsilon_3 V_4 + 12\kappa_1 \kappa_1'^3 V_1 V_5 \\
&\quad + 72\kappa_1 \kappa_1'^3 \upsilon_2 V_5 + 12\kappa_1 \kappa_1'^3 V_6 + 4\kappa_1 \kappa_1'^3 \upsilon_7 + 24(2\kappa_1 \kappa'_1 \kappa'_2 + \kappa_1'^2 \kappa_2) V_2^2 + 6(2\kappa_1 \kappa'_1 \kappa'_2 + \kappa_1'^2 \kappa_2) V_1 V_3 \\
&\quad + 2(2\kappa_1 \kappa'_3 + 2\kappa'_1 \kappa_3 + 3\kappa_2 \kappa'_2) V_2 + 48\kappa_1'^4 \upsilon_2 V_2^3 + 48\kappa_1'^4 V_1 V_2^3 + 48\kappa_1'^4 V_1 V_3^2 + 240\kappa_1'^4 \upsilon_2 V_3^2 \\
&\quad + 32\kappa_1'^4 \upsilon_4 V_4 + 288\kappa_1'^4 V_2^2 V_3 + 24\kappa_1'^4 V_1^2 V_2 V_3 + \kappa_1'^4 V_1^3 V_4 + 144\kappa_1'^4 \upsilon_4 V_2^2 + 72\kappa_1'^4 V_1 V_2 V_4 \\
&\quad + 128\kappa_1'^4 V_3 V_4 + 4\kappa_1'^4 V_1^2 V_5 + 72\kappa_1'^4 V_2 V_5 + 56\kappa_1'^4 \upsilon_3 V_5 + 6\kappa_1'^4 V_1 V_6 + 24 V_2 V_6 \kappa_1'^4 \upsilon_2 V_6 + 4\kappa_1'^4 V_7 \\
&\quad + \kappa_1'^4 \upsilon_8 + 36\kappa_1'^2 \kappa'_2 V_1 V_2^2 + 6\kappa_1'^2 \kappa'_2 V_1^2 V_3 + 4\kappa'_1 \kappa'_3 V_1 V_2 + 3\kappa_2'^2 V_1 V_2 + \kappa'_4 \upsilon_2 \,.
\end{aligned}
$$

Proton Number Fluctuations

Reduced Proton Cumulants (Fully Corrected)